

Serveur Académique Lausannois SERVAL serval.unil.ch

Author Manuscript

Faculty of Biology and Medicine Publication

This paper has been peer-reviewed but does not include the final publisher proof-corrections or journal pagination.

Published in final edited form as:

Title: Central Metabolic Responses to Ozone and Herbivory Affect Photosynthesis and Stomatal Closure.

Authors: Papazian S, Khaling E, Bonnet C, Lassueur S, Reymond P, Moritz T, Blande JD, Albrechtsen BR

Journal: Plant physiology

Year: 2016 Nov

Issue: 172

Volume: 3

Pages: 2057-2078

DOI: 10.1104/pp.16.01318

In the absence of a copyright statement, users should assume that standard copyright protection applies, unless the article contains an explicit statement to the contrary. In case of doubt, contact the journal publisher to verify the copyright status of an article.

1 **Central Metabolic Changes to O₃ and Herbivory in *B. nigra* Affect Photosynthesis**
2 **and Stomata Closure**

3
4 Running title: Omics Multiple Stress Responses in *Brassica nigra*

5
6 Stefano PAPAZIAN^a, Eliezer KHALING^b, Christelle BONNET^c, Steve LASSUEUR^c,
7 Philippe REYMOND^c, Thomas MORITZ^d, James D. BLANDE^{b,1}, Benedicte R.
8 ALBRECHTSEN^{a,1}

9
10 ^{a.} Umeå Plant Science Centre, Department of Plant Physiology, Umeå University, 90187
11 Umeå, Sweden

12 ^{b.} Department of Environmental and Biological Sciences, University of Eastern Finland,
13 P.O. Box 1627, FIN-70211, Kuopio, Finland.

14 ^{c.} Department of Plant Molecular Biology, University of Lausanne, 1015 Lausanne,
15 Switzerland

16 ^{d.} Umeå Plant Science Centre, Department of Forest Genetic and Plant Physiology,
17 Swedish University of Agricultural Sciences, 90187 Umeå, Sweden

18
19 ¹Address correspondence to:

20 Benedicte Albrechtsen benedicte.albrechtsen@umu.se

21 and James Blande james.blande@uef.fi

22
23
24

25 One sentence summary:

26 When facing a scenario of sequential abiotic and biotic stress, black mustard regulates
27 glycerol and central energy metabolism to prioritize processes of photosynthesis and
28 stomatal osmoregulation.

29

30 **ABSTRACT**

31 Plants evolved adaptive mechanisms which allow them to encounter a continuous range
32 of abiotic and biotic stressors. Tropospheric ozone (O₃) is a global anthropogenic
33 pollutant that directly affects living organisms and ecosystems, including plant-herbivore
34 interactions. In this study we investigate the stress responses of the wild black mustard
35 (*Brassica nigra*) exposed consecutively to O₃ and the specialist herbivore *Pieris*
36 *brassicae*. Transcriptomics and metabolomics data were evaluated via multivariate,
37 correlation and network analyses for the O₃ and herbivory responses. O₃ stress
38 symptoms resembled those of senescence and phosphate starvation, while sequential
39 shift from O₃ to herbivory induced characteristic plant defense responses, including
40 decrease in central metabolism, induction of the JA/ET pathways, and emission of
41 volatiles. Omics network and pathway analyses predicted a link between glycerol and
42 central energy metabolism, with impact on processes of osmotic stress response and
43 stomatal closure. Further physiological measurements confirmed that, while O₃ stress
44 inhibited photosystem and carbon assimilation, sequential herbivory counteracted the
45 initial responses induced by O₃, resulting in a phenotype which was similar to the one
46 observed after herbivory alone. Overall, this study addresses the consequences of
47 multiple stress interactions on a plant metabolic system, but it also represents an
48 example of how omics data can be integrated to generate new hypotheses in ecology
49 and plant physiology.

50

51 INTRODUCTION

52 Under natural conditions plants are continuously exposed to abiotic and biotic stresses.
53 When studied in the laboratory, individual stresses trigger a variety of molecular, cellular,
54 and physiological responses (**Ben Rejeb et al., 2014; Suzuki et al., 2014**). However,
55 the way plants protect themselves in nature cannot be predicted on the basis of
56 responses to individual stresses alone, as combined stresses may elicit antagonistic,
57 neutral, or synergistic effects (**Rizsky et al., 2002, 2004; Mittler, 2006; Pandey et al.,**
58 **2015**). Thus, there is increasing interest in plant responses to multiple stress conditions,
59 and while most studies have focused on multiple abiotic factors (**Suzuki et al., 2014**),
60 biotic factors are usually limited to pathogen infection (**Sharma et al., 1996; Xiong and**
61 **Yang, 2003; Anderson, 2004; Prasch and Sonnewald, 2013**; but see **Atkinson and**
62 **Urwin, 2012; Atkinson et al., 2013**).

63 Global warming encompasses a range of interrelated abiotic phenomena, including
64 increases in the Earth's average temperature and changes in the greenhouse gas [e.g.
65 methane, carbon dioxide (CO₂), and ozone (O₃)] composition of the atmosphere.
66 Burning of fossil fuels releases nitrogen oxides and hydrocarbons, which in the presence
67 of sunlight react to form tropospheric O₃, the most significant pollutant in the atmosphere
68 in terms of phytotoxicity (**Ludwikow and Sadowski, 2008; Renaut et al., 2009; Van**
69 **Dingenen et al., 2009**). Plant responses to O₃ vary according to the intensity and
70 duration of the exposure, but generally concur with deleterious effects on plant fitness,
71 disturbing the processes of photosynthesis, energy and carbon metabolism, cellular
72 detoxification, and transpiration (**Bagard et al., 2008; Dizengremel et al., 2008; Fares**
73 **et al., 2010; Goumenaki et al., 2010; Salvatori et al., 2015**). However, while acute

74 exposure to high O₃ levels can rapidly cause induction of cell death and chlorosis (for
75 reviews see **Ashmore 2005; Kangasjärvi et al., 2005; Vainonen and Kangasjarvi,**
76 **2015**), negative yield responses are not always correlated with the severity of symptoms
77 in leaves, and exposure to O₃ can affect the plant metabolic processes prior to any
78 visible injury (**Long and Naidu 2002; Dizengremel et al., 2009; Sawada & Kohno,**
79 **2009; Pinto et al., 2010**).

80 Damage to plants caused by herbivory is also predicted to increase in response to
81 global change, either through direct effects on the herbivore behavior and survival, or
82 through indirect effects on the host plant condition (**Bale et al., 2002; Fuhrer, 2003;**
83 **Ditchkoff et al., 2009; Lindroth, 2010; Khaling et al., 2015**). Negative effects of
84 herbivory and defoliation on plant fitness include systemic down-regulation of
85 photosynthesis and reduced CO₂ assimilation (**Zangerl et al., 2002; Hui et al. 2003;**
86 **Ralph et al., 2006; Tang et al., 2006**). Thus, to protect against herbivores, plants
87 evaluate priorities and allocate resources between growth and defense (**Koricheva,**
88 **2002; Schwachtje and Baldwin, 2008; Firn and Jones, 2009; Havko et al., 2016**).

89 In Brassicaceae, leaf-chewing herbivores activate phytohormone signaling, where
90 crosstalk between JA and ET pathways fine-tunes the defense response (**de Vos et al.,**
91 **2005; Pieterse et al., 2012**). The large cabbage white (*Pieris brassicae*) is a specialist
92 Brassicaceae-feeding herbivore and is an important pest of black mustard (*Brassica*
93 *nigra*). *P. brassicae* oviposition on the host plant is influenced by glucosinolates (sulfur
94 and nitrogen containing glucosides) that function as chemical cues for the butterfly
95 (**Fahey et al., 2001; Petersen et al., 2002; Halkier and Gershenzon, 2006; Textor and**
96 **Gershenzon, 2008**). Young caterpillars primarily feed on mature leaves of *B. nigra*, but

97 after the third instar they move to fresh tissues with higher glucosinolate content, such
98 as flowers and buds (**Smallegange et al., 2007**). Plant-herbivore interactions are thus
99 frequently described with an emphasis on specialized (secondary) metabolism
100 (**Simmonds, 2003; van Dam et al., 2004; Poelman et al., 2010; Boeckler et al., 2011;**
101 **Lof et al., 2013; Onkokesung et al., 2014**). However, plant metabolism has a large
102 functional overlap between growth and defense traits, and reconfiguration at the level of
103 primary and energy metabolism can play a central role in the processes of stress
104 tolerance, signal transmission, and direct defense (**Both et al 2005; Rolland et al.,**
105 **2006; Schwachtje and Baldwin 2008; Fernandez et al., 2010**).

106 The metabolomics approach has already been applied to different areas of plant biology
107 and ecology (for reviews see **Sardans et al., 2011** and **Weckwerth, 2011**), where it has
108 helped in understanding the regulation of pathways during plant-herbivore interactions
109 (**Jansen et al., 2008; Misra et al., 2010**) and plant stress responses (**Shulaev et al.,**
110 **2008; Nakabayashi and Saito, 2015**). What typically distinguishes metabolomics from
111 targeted analyses, or general metabolic profiling, is the ambition to integrate with other
112 omics sciences (**Fiehn, 2002; Barah and Bones, 2014**). Combined with the ‘guilt-by-
113 association’ principle (**Bino et al., 2004; Saito et al., 2008**), omics analyses allow
114 prediction of unknown gene and metabolite functions. For instance, the systematic
115 metabolomics approach has been successful in determining the biosynthetic regulation
116 of glucosinolates by MYB transcription factors (**Hirai et al., 2007; Sønderby et al., 2007**)
117 and in the modelling of the costs of glucosinolate biosynthesis in terms of primary
118 metabolism (**Bekaert et al., 2012**). New hypotheses generated by this data driven (“top-
119 down”) strategy can thus guide the understanding of regulatory and metabolic pathways,

120 and eventually predict the emergence of certain phenotypes (**Fukushima et al., 2009;**
121 **Saito and Matsuda, 2010**).

122 Through integrated transcriptomics and metabolomics analyses in our study, we sought
123 to understand the systems regulation of *B. nigra* when exposed to sequential stress by
124 O_3 and *P. brassicae* herbivory. We found that shift from abiotic to biotic stress responses
125 differentially regulated glycerol and energy metabolic networks. In our model, these
126 pathways were functionally associated with photosystem and mitochondrial activity, and
127 were further predicted to involve physiological responses related to osmotic stress
128 tolerance and stomatal closure. Altogether, these results suggest an important role of
129 these central processes in the plant adaptation to sequential abiotic and biotic stresses.
130 The impact of the stresses on the plant physiology was assessed in an additional
131 experiment with measurements of photosynthesis and gas exchange, which confirmed a
132 negative effect of *P. brassicae* herbivory on the plant ability to regulate stomatal closure
133 and transpiration in response to O_3 .

134

135

136 RESULTS

137 Black mustard was subjected to the following stress scenarios: O₃ fumigation at 70 ppb
138 for five days (O); herbivore-feeding by first instar *P. brassicae* caterpillars for 24 hours
139 (P); exposure to O₃ followed by herbivory (OP). Leaf samples were shared for omics
140 analyses (**Figure 1**: “Experiment 1”). Transcriptomics screening was based on
141 *Arabidopsis* CATMAv4 whole-genome microarrays (**Sclep et al., 2007**), while
142 metabolomics screening combined GC-MS, LC-MS, and VOCs collected via dynamic
143 headspace sampling and analysed by GC-MS (See **Supplemental Datasets S1** and
144 **S2**). Omics data were first examined separately and then integrated via network and GO
145 analyses. Molecular and metabolic responses were framed in a model which predicted
146 opposite regulatory dynamics between O₃ and sequential herbivory. This hypothesis was
147 tested in a follow-up experiment (**Figure 1**: “Experiment 2”), where physiological data of
148 chlorophyll content, photosynthesis rate, and gas exchange, were measured for the
149 same stress conditions (O, P, OP), and for a long term O₃ exposure of 16 days (OL).

150

151 Transcriptome Responses

152 Hierarchical cluster and gene ontology (GO) analyses of 970 differentially expressed
153 genes (P -value < 0.05) (**Figure 2A, 2B**) separated the O₃ stress treatment (O) from
154 herbivory (P) and the sequential stress treatment (OP). After GO enrichment, the
155 strongest response was represented by energy metabolic processes, including
156 photosystem and the mitochondria electron transport chain (ETC) (**Figure 2A, 2B**).
157 Overall, expressions in O were highly homogenous (Pearson’s coefficient, ρ = 0.6-0.8),
158 while P and OP showed lower correlation within their clusters (ρ = 0.2-0.5; **Figure 2C**).
159 MapMan pathway analysis confirmed similar responses at several biological levels

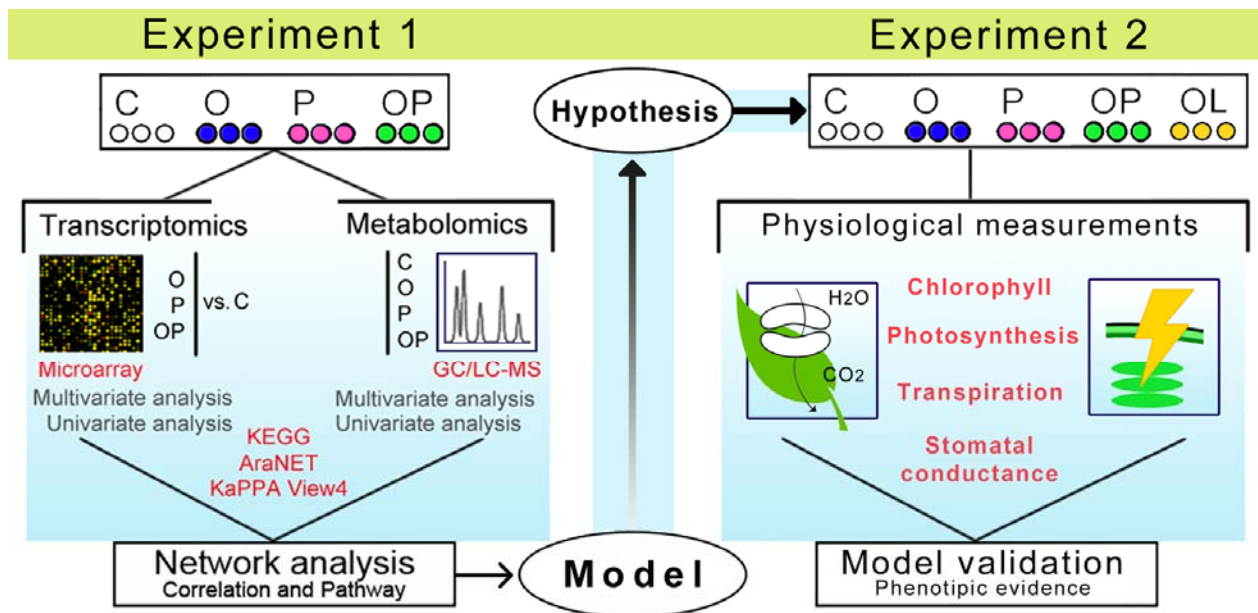


Figure 1. Design of omics experiments, hypothesis generation and validation via physiological evidence. Experiment 1: five weeks old *Brassica nigra* plants were exposed to abiotic and/or biotic stresses, including O₃ fumigation at 70 ppb for five days (O), herbivore-feeding with 30 first instar *P. brassicae* caterpillars for 24 hours (P), sequential stress of O₃ followed by herbivore-feeding (OP), or no treatment as controls (C). To obtain a comprehensive understanding of metabolome and transcriptome responses to the treatments, leaves of equal developmental stage were sampled from the same plants from which volatile emissions (VOCs) had been obtained. Statistical and network analyses combined omics data in a model which connected the metabolic responses with physiological adaptation to the multiple stress condition. *B. nigra* responses were further evaluated in Experiment 2: physiological parameters were measured for the same stress treatments (O, P, OP) and for a long term exposure to O₃ at 70 ppb for 16 days (OL). The initial hypothesis was thus verified through validation of the omics model, which predicted differential physiological responses of photosystem, carbon assimilation and stomatal regulation.

160 (Figure 2D), while Venn diagrams based on Log₂ fold changes ≥ 0.585 (for P -value <
 161 0.05) indicated a dominance of up- and down- regulated genes in O, with the least
 162 impact in OP (Figure 2E).
 163 Genes involved in photosystem and carbon assimilation were down-regulated in
 164 response to all stress scenarios but particularly in O (Figure 2D, 2F), which also
 165 resulted in up-regulation of non-photochemical quenching *NPQ1* (Figure 2F). Other
 166 primary processes such as amino acid and carbohydrate metabolism generally showed
 167 opposite patterns of regulation for O₃ and herbivory (Figure 2D, 2G). In the sequential
 168 treatment (OP), *B. nigra* activated defense responses characteristic to herbivory alone

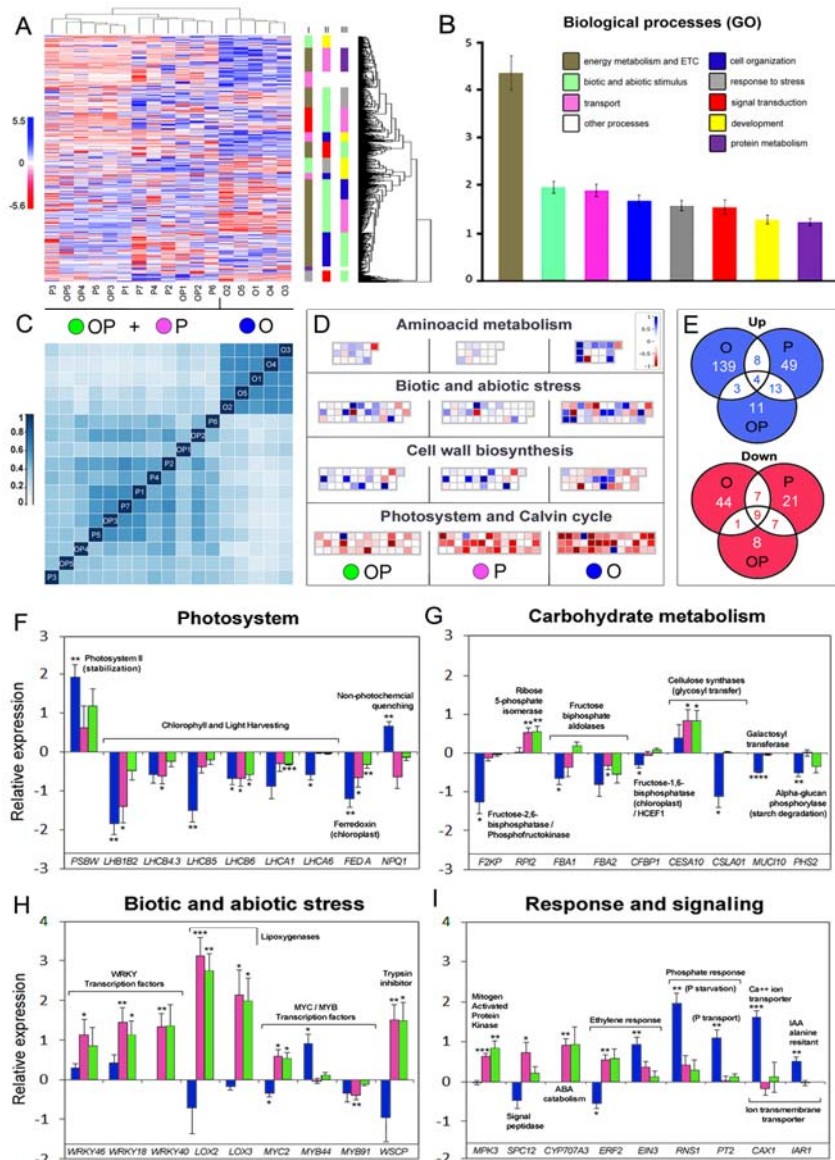


Figure 2. Transcriptome responses in *B. nigra* under multiple O₃ and herbivory stress treatments: O₃ stress (O), herbivory by *P. brassicae* (P), sequential treatment (OP). A, Heat-map for expression profiles of 970 genes, P-value ≤ 0.05 (rows) versus samples (columns) sorted by hierarchical clustering. Red indicates down-regulation, and blue up-regulation. GO enriched biological processes for each cluster was ranked (I, II, III) for their relative abundance and colored as in B. Summary of total GO processes significantly enriched in all the gene clusters, ordered by their relative abundance (for all 970 genes). C, Heat-map of Pearson's correlation coefficient (ρ) as calculated for each sample pairs from the corresponding hierarchical clustering; darker blue shade indicates higher correlation ρ . D, Mapman biological functions (bins) showing the effect of the stress treatments on gene expression relative to amino acid metabolism, biotic and abiotic stress, cell wall biosynthesis, photosystem and Calvin cycle. E, Venn-diagrams (MapMan generated) comparing genes up- and down-regulated in response to the treatments, for Log₂ fold-change thresholds > 0.585 (P-value ≤ 0.05). Lower panels show univariate analysis relevant to regulation of central metabolism and stress responses: F, processes of photosystem and light harvesting. G, carbohydrate metabolism. H, biotic and abiotic stress. I, response and signaling. Relative expressions are reported as log₂ values. Significance relative to the controls (zero-level) is reported as student t-test P-values of * ≤ 0.05 , ** ≤ 0.01 , *** ≤ 0.001 , **** ≤ 0.0001 . Error bars= S.E. Treatments: ozone (O) in white; herbivory by *P. brassicae* (P) in grey; sequential treatment (OP) in black.

169 (P) (Figure 2H, 2I) - e.g. lipoxygenases *LOX2* and *LOX3* (Felton et al., 1993;
 170 Halitschke and Baldwin, 2003), trypsin inhibitor *WSCP* (Zavala and Baldwin, 2004;
 171 Boex-Fontvieille et al., 2015) and mitogen-activated protein kinase *MPK3* (Pitzschke

172 **and Hirt, 2008**). Notably, genes involved in stress responses and phytohormone
173 signaling were differentially regulated for the single O₃ stress and the herbivory
174 treatments (e.g. *WRKYs*, *MYC2*, *ERF2*), and only in O were abiotic stress responses
175 induced, such as drought (*MYB44*), senescence (*EIN3*), and phosphate starvation
176 (*RNS1*, *PT2/PHT1.4*) (**Figure 2H, 2I**).

177

178 **Metabolome Responses**

179 A multivariate analysis of the metabolome profile explained 65% of the metabolic
180 variation, and 95% of the treatment effects (PLS-DA, **Figure 3A, Supplemental Figure**
181 **S1 and Supplemental Table S1**). Both O₃ stress and herbivory caused a shift from the
182 basal metabolic state of the untreated plants, inducing unique profiles as single
183 treatments in O and P. However, the effect of herbivory largely overshadowed the effect
184 of O₃ in the sequential treatment OP, indicated by the swarm overlap with P (**Figure 3A**).
185 Despite the importance of several metabolite pools in the multivariate model (**Figure 3B**
186 and **Supplemental Table S2**; 70 compounds for VIP scores > 1.00), single univariate
187 effects were only confirmed for a subset of these (**Figure 3C**, ANOVA post-hoc Tukey
188 tests).

189 Opposite effects of O₃ and herbivory were observed on pools of primary metabolites -
190 sugars, amino acids, and organic acids - which increased in O and decreased in P and
191 OP (**Figure 3B and Supplemental Table S2**). However, a common response to all
192 treatments was a three-fold induction of γ -aminobutyric acid (GABA; **Figure 3B, 3C**),
193 which partly correlated with its precursor α -ketoglutarate (α -KG) (**Figure 3B**). Most
194 noticeably, glycerol increased to 155% in O (**Figure 3B, 3C**), but was restored to steady-
195 state levels in the sequential treatment OP. A similar trend was observed for

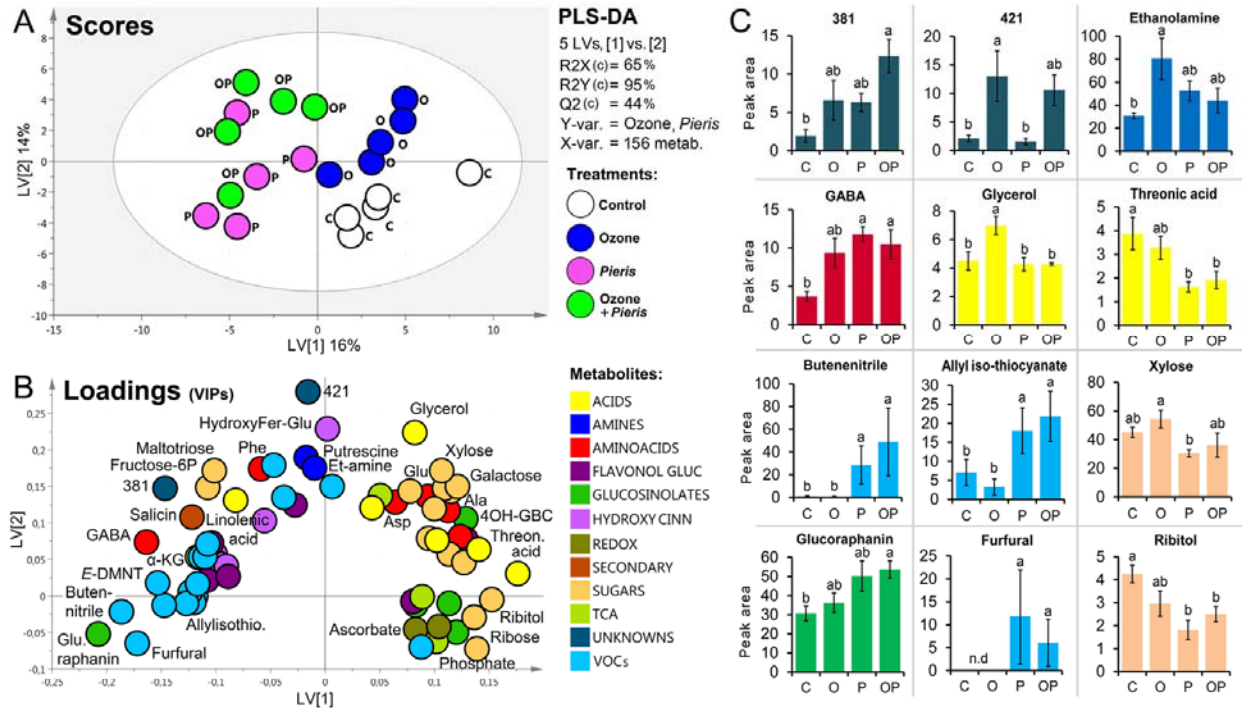


Figure 3. Metabolome responses in *B. nigra* under multiple O₃ and herbivory stress treatments. O₃ stress (O), herbivory by *P. brassicae* (P), sequential treatment (OP), and untreated plants (C). Leaf bound metabolites were analysed through LC-MS and GC-MS, while VOCs were collected via head-space and analysed with GC-MS. Five LVs cumulatively explained 65% variation in X (R²X[c]), and 95% of the treatment response (R²[c]Y), with 44% of total model predictability (Q²[c]). See model statistics and metabolite identities in Supplemental Table S1 and S2. A, PLS-DA score plot of first and second latent variables, [LV1] vs. [LV2]. See Supplemental Fig S1 for score plots relative to [LV3]. B, PLS-DA loading plot showing important metabolites for the model (VIPs > 1.00). C, ANOVAs with post-hoc Tukey comparisons to test treatment effects for selected compounds (different letters indicate different response means). Error bars = SE.

196 ethanolamine, another metabolite of the glycerophospholipid pathway and a component
 197 of lipid membranes (**Figure 3C**). Phenolic compounds, such as flavonols and cinnamic
 198 acid ester derivatives (**Lin et al, 2011; Shao et al., 2014**) increased in all treatments.
 199 Glucosinolate levels were stable or reduced (with glucoraphanin the only exception),
 200 while VOCs were emitted upon herbivore damage (P, OP), including glucosinolate
 201 derivatives and green leaf volatiles (GLVs) (**Figure 3B, 3C** and **Supplemental Table**
 202 **S2**). Two unidentified secondary compounds, previously described by **Khaling et al.**
 203 **2015** (i.e. “421” [M-H]⁻ m/z 485.13, and “381” [M-H]⁻ m/z 349.15), were also induced,
 204 confirming their importance respectively in O and OP (**Figure 3C**).

205

206 Omics Integrative Network Correlation Analysis

207 Transcriptomic and metabolomic profiles were integrated in a scale-free correlation
208 network (**Figure 4**) (see topology in **Supplemental Figure S2**). The network was
209 dominated by assortative high-degree nodes (*hubs*), with major hubs involved in
210 processes such as stress signaling, cellulose biosynthesis, chloroplast activity and
211 stomatal regulation (**Table I**). Several primary metabolites clustered around the central
212 region of the network, while distinct modules of secondary metabolites clustered at the
213 periphery – i.e. glucosinolates, flavonol glucosides, hydroxycinnamic acid derivatives,
214 and VOCs (**Figure 4A-C**). Most glucosinolates connected to *CYP71*, a cytochrome
215 involved in herbivore-induced responses and formation of nitriles (At5g25120 /
216 At5g25180; **Bennett et al., 1993, Irmisch et al., 2014**). Glucobrassicin and
217 neoglucobrassicin (indolics) directly clustered with VOCs (nitriles and GLVs) and
218 positively correlated with *WRKY40* (involved in indolic glucosinolate biosynthesis and
219 GLV emissions; **Schön et al., 2013; Mirabella et al., 2015**), *WRKY46* and *CYP707A3*
220 (both involved in ABA metabolism; **Saito et al., 2004; Liu et al., 2012; Geilen and**
221 **Bohmer, 2015**) (**Figure 4C**). The herbivory response (P) linked to glycerol via four
222 nodes, including two genes coding for flavin monooxygenases *NOGC1* (At1g62580) and
223 *FMO* (At1g12200), which negatively correlated with glycerol ($\rho = -0.86$, P -value < 0.001)
224 and positively correlated with each other ($\rho = 0.85$, P -value < 0.001) (**Figure 4A, 4B**).
225 *MYB44* linked to the same module and negatively correlated with *NOGC1* ($\rho = -0.91$, P -
226 value < 0.0001) while it positively correlated with glycerol ($\rho = 0.68$, P -value =
227 0.006)(**Figure 4B**). Notably, both *MYB44* and *NOGC1* are involved in osmotic stress
228 response and regulation of stomatal closure.

229

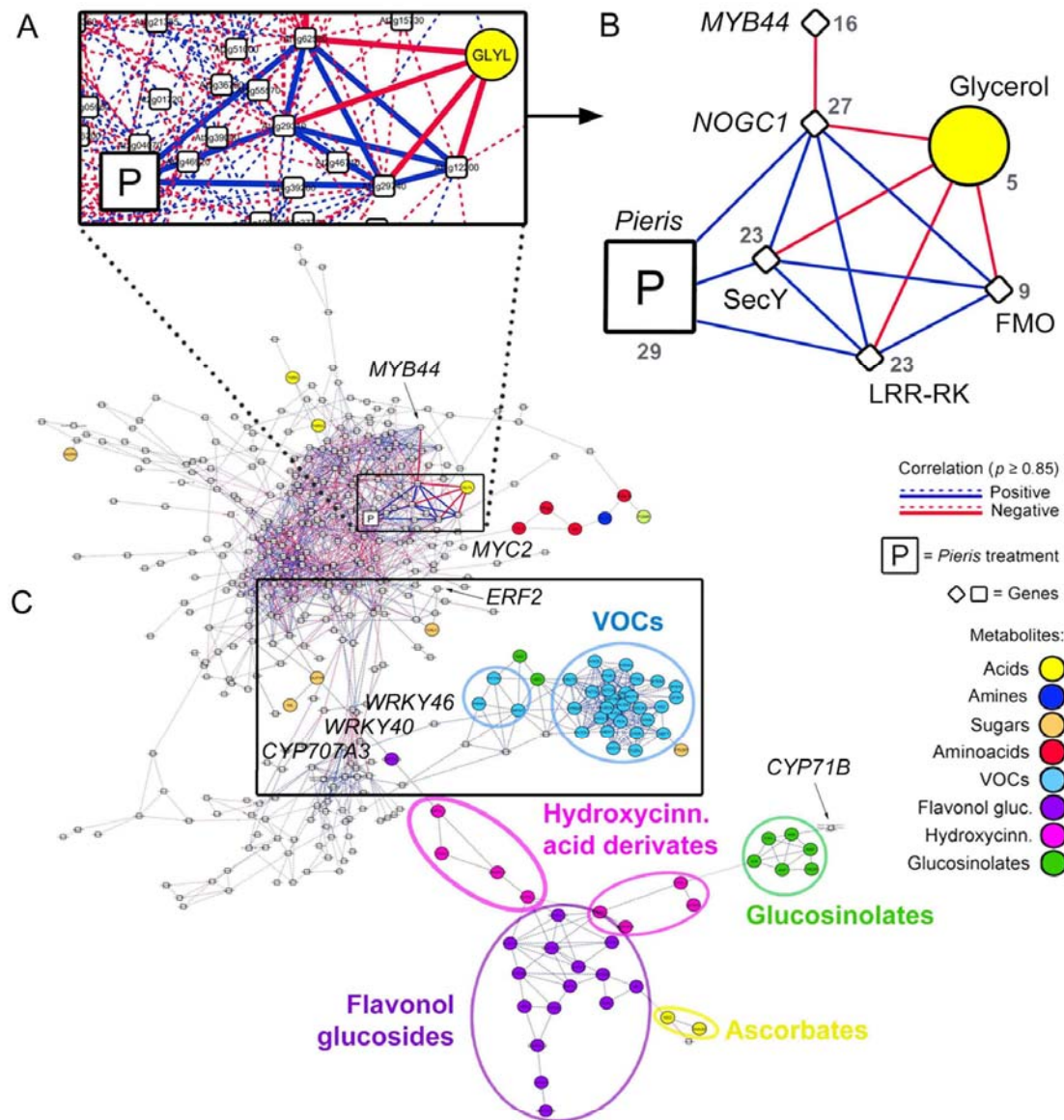


Figure 4. Omics integrative network correlation analysis for multiple stress responses in *B. nigra*. Gene expression profiles for 970 genes (P-value < 0.05) were correlated with the metabolome profile (156 compounds) considering all the treatments conditions of O3 stress and *P. brassicae* herbivory. The resulting graph was rendered as a network which was generated in Cytoscape. Edges: Pearson's correlation coefficient ($p \geq 0.85$) for positive (blue) and negative (red) correlation. Nodes: genes (white squares/diamonds), metabolites (colored circles). Herbivore variable for the effect of *P. brassicae* treatment is indicated by the bold letter (P), white square. A, Network of gene-to-gene, gene-to-metabolite, and metabolite-to-metabolite correlations. B, Zoom-in on the gene-to-metabolite subnet highlighting the effect of (P) on glycerol and co-expressed genes (MYB44, flavin monooxygenases NOGC1 and FMO, a LRR-RK receptor and a SecY protein). C, VOCs subnet, connecting central metabolism to secondary metabolism (glucosinolates, hydroxycinnamic acid derivatives and flavonol glucosides) via WRK40, WRK46, and CYP707A3.

230 Responses Relative to Energy and Glycerol Metabolic Networks

231 Energy metabolic processes (photosystem and mitochondria) were the most affected by
 232 the stress treatments (**Figure 2A, 2B**). Based on these energy genes (functionally

Energy metabolism

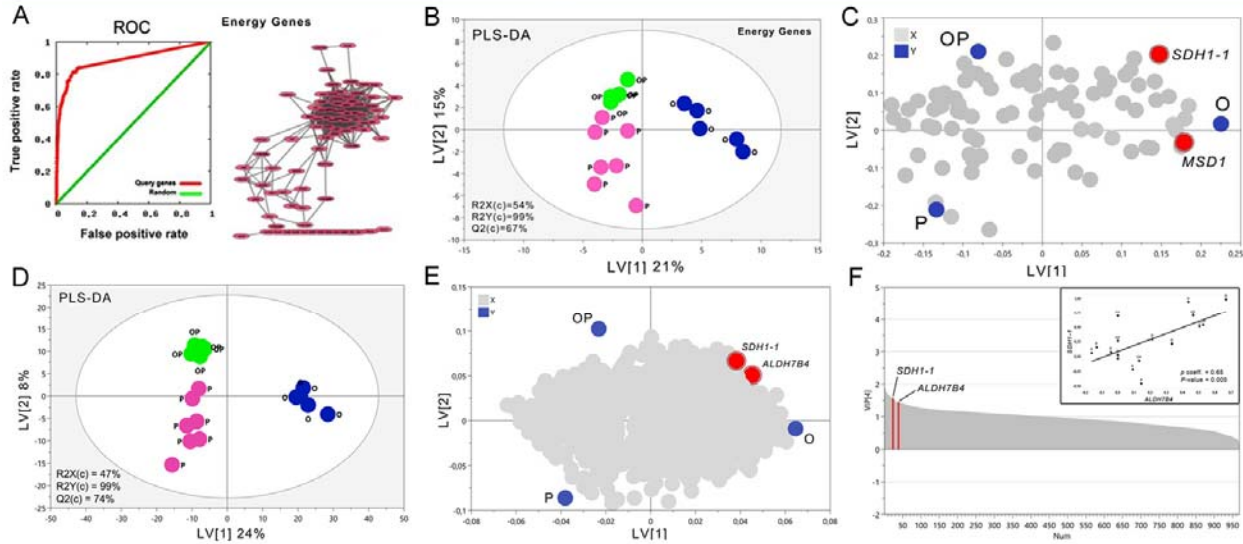


Figure 5 Regulation of energy metabolic networks in *B. nigra*, under multiple O₃ and herbivory stress treatments. A, Network model (AraNet) assessing gene connectivity between the 85 genes enriched in energy metabolic processes. Model fitness was calculated by genes inter-connectivity of the receiver operating characteristic (ROC), for true-positives and false-positives rate between the entry genes (red curve) and a randomly generated gene-set (green curve). The network scored high area under the curve (AUC = 0.89; P-value = 1.82 E-62). B-C, Multivariate analysis evaluating the change in expression of energy genes in the network, during the multiple stress treatments: O₃ (O), herbivory by *P. brassicae* (P), and sequential treatment (OP). PLS-DA score and loading plots of first and second latent variables [LV1] vs. [LV2] are shown. Treatments: O, P and OP. Five LVs cumulatively explained 54% variation in X (R2X[c]), and 99% of the treatment response (R2[c]Y), with 67% of total model predictability (Q2[c]). The importance of mitochondrial genes *SDH1-1* and *MSD1* in the model is highlighted (in red; VIP = 1.40 and 1.34; see in Supplemental Table S4 and S5). D-E, Multivariate analysis for general model (970 genes; P-value ≤ 0.05). Treatments: O, P, and OP. PLS-DA score and loading plots of first and second latent variables [LV1] vs. [LV2] are shown (see Supplemental Table 6 and 7). In red, *SDH1-1* (VIP = 1.57) and *ALDH7B4* (VIP = 1.45), are important for O₃ treatments (O, OP), as also shown in F, distribution of VIP values for all 970 genes, and correlation between expression of *SDH1-1* and *ALDH7B4* throughout all treatment conditions, Pearson's coefficient (ρ) = 0.65, P-value = 0.005.

233 connected in AraNet; **Figure 5A**), a PLS-DA strongly separated the stress treatments O,
 234 P and OP, explaining 54% of the variation in gene expression, and 99% of the
 235 treatment effects (**Figure 5B** and **Supplemental Table S4**). In response to O₃ stress,
 236 the mitochondrial ETC Complex II succinate dehydrogenase subunit *SDH1-1*
 237 (*At5g66760*) and the mitochondrial superoxide dismutase *MSD1* (*At3g10920*), were both
 238 up-regulated (**Figure 5C**, **Supplemental Table S5**). In the general model for expression
 239 of all 970 genes (**Figure 5D**, **5E**, and **Supplemental Table S6** and **S7**), *SDH1-1* again
 240 strongly described the effect of O₃ (O, OP) while it positively correlated with *ALDH7B4*

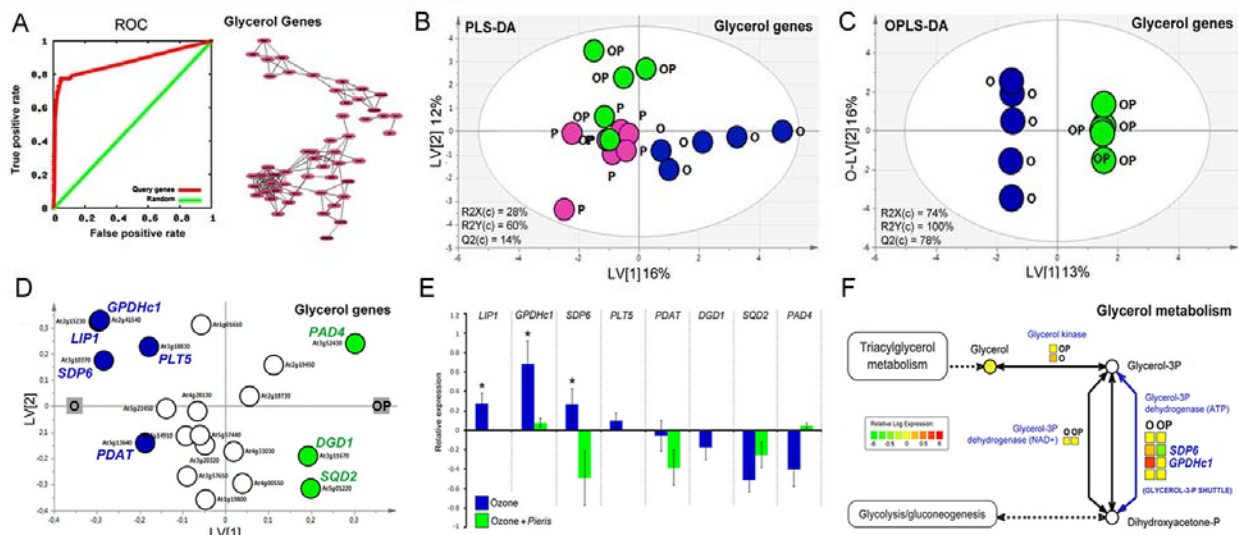
241 (At1g54100; Pearson's coefficient $\rho = 0.65$, P -value = 0.005; **Figure 5E, 5F**), aldehyde
242 dehydrogenase involved in glycerol metabolism.

243 Visualization of the entire glycerolipid pathway in KEGG/KaPPA-View4 confirmed up-
244 regulation in O of *ALDH7B4* (P -value = 0.005; **Supplemental Figure S5**) and of the
245 adjacent aldo-keto reductase *AKR4C10* (At2g37790; P -value < 0.05), which together
246 with *ALDH7B4* reversibly converts glycerate into glyceraldehyde and glycerol (see paths
247 in **Supplemental Figure S6 and S7**). Interestingly, both *AKR4C10* and *ALDH7B4* are
248 involved in oxidative and osmotic stress tolerance during abiotic and biotic responses
249 (**Kotchoni et al. 2006, Missihoun et al., 2014; Sengupta et al., 2015**).

250 On the basis of genes annotated for GO enzyme substrate "glycerol-" (**Supplemental**
251 **Table S8**) which functionally connected in AraNet (**Figure 6A**), a PLS-DA could
252 separate the treatments O from P and OP, explaining 28% of the variation in gene
253 expression, and 60% of the treatment effects (**Figure 6B and Supplemental Table S9**).

254 In an OPLS-DA, the single and sequential O₃ treatments (O, OP) could be further
255 divided by the activity of eight genes (VIP > 1.00): *LIP1*, *GPDHc1*, *SDP6*, *PLT5*,
256 *PDAT*, *DGD1*, *SQD2*, and *PAD4* (**Figure 6C, 6D**; see model statistics in **Supplemental**
257 **Table S10**). Particularly, the triacylglycerol lipase *LIP1* (At2g15230; fatty acids
258 catabolism, **Ei-Kouhen et al., 2005**) was up-regulated in O compared to OP (P -value <
259 0.05; **Figure 6E, 6F**), while the sulfolipid synthase *SQD2* (At5g01220; biosynthesis of
260 photosynthetic membranes components) was significantly down-regulated in O (P -value
261 = 0.02) but not in OP (**Figure 6E, 6F** and KEGG/KaPPA View4 paths in **Supplemental**
262 **Figure S6 and S7**). Moreover, the glycerol 3-phosphate (G3P) dehydrogenases
263 *GPDHc1* and *SDP6* (At2g41540 and At3g10370; **Shen et al., 2006**) were both up-
264 regulated in O and negatively affected by herbivory in OP (P -value < 0.05; **Figure 5E**).

Glycerol metabolism



265 Pathway visualization in KEGG/KaPPA-View4 (**Figure 6F**) showed that *GPDHc1* and
 266 *SDP6* (respectively located in the cytosol and on the mitochondrial membrane)
 267 constitute the G3P shuttle which is responsible for transport of reducing equivalents to
 268 the mitochondrial ETC via recycling of dihydroxyacetone phosphate (**Shen et al., 2003**;
 269 **Shen et al., 2006; Quettier et al., 2008**).

270

271 Predictive Interactions of GO Functional Networks

272 During shift between O₃ stress and herbivory, *B. nigra* actively regulated energy and
 273 glycerol metabolic processes (**Figure 2, 3, 5, 6**), possibly in connection with osmotic

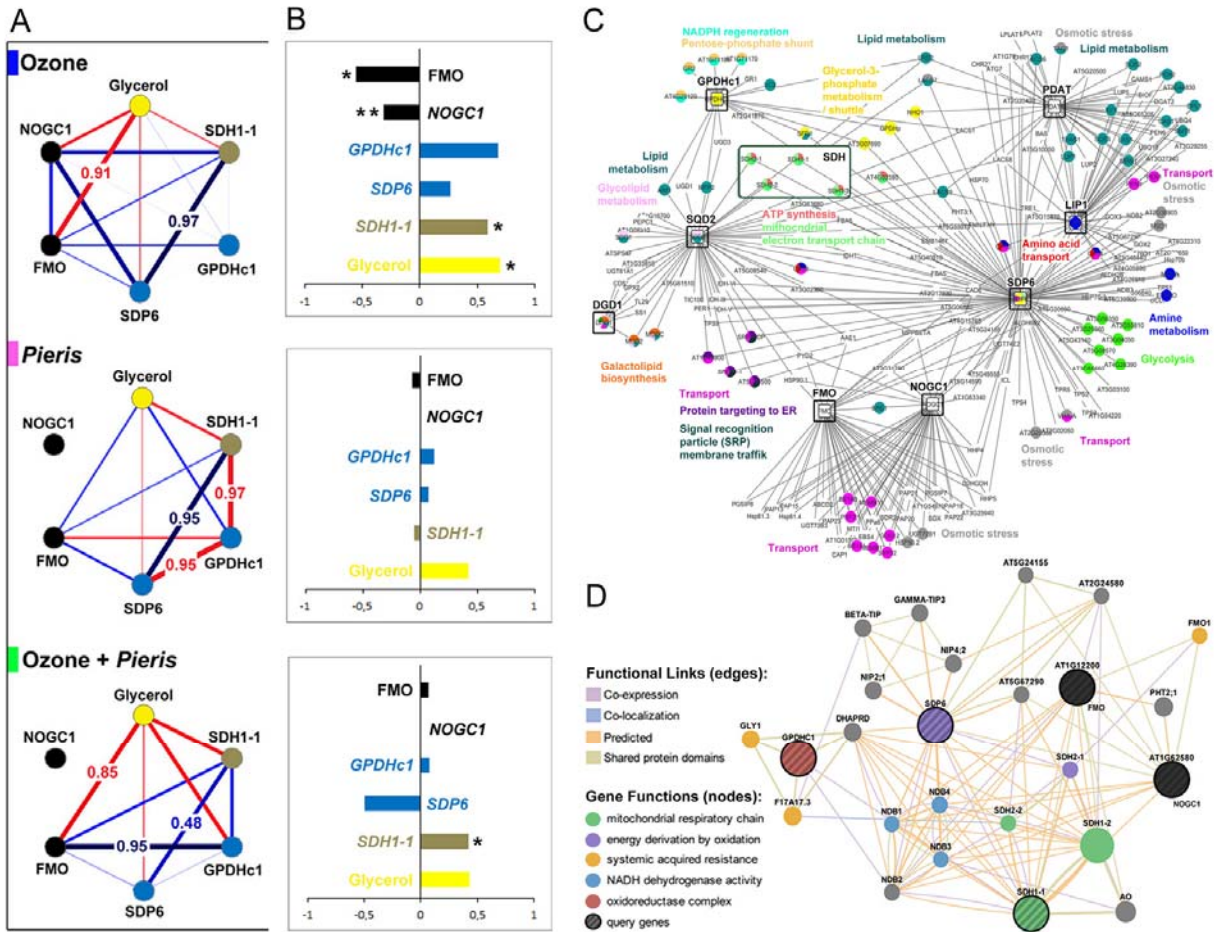


Figure 7 Components of glycerol metabolic network and mitochondrial ETC, under multiple O₃ and herbivory stress treatments. Comparative correlation analysis and predictive GO network interactions (AraNet and GeneMANIA). **A**, Comparative correlation analysis between glycerol, components of G3P shuttle (GPDHc1 and SDP6), mitochondrial ETC Complex II (SDH1-1), and flavin monooxygenases (NOGC1 and FMO). Treatments: O, P and OP. Edges indicate Pearson's coefficient (ρ) for positive (blue) and negative (red) correlations. All correlation values reported were significant (between P-value < 0.05 and < 0.001), beside the two correlations in the sequential (OP) of glycerol/FMO ($\rho = 0.85$), and SDP6 /SDH1 ($\rho = 0.48$) which were not significant. **B**, Average of relative gene expressions (Log₂), and glycerol abundance, for each treatment (O, P, OP) and corresponding student t-test significance (P-value = * < 0.05 , ** < 0.01) when compared to the control conditions. **C**, Gene interactions predicted in AraNet, for the glycerol metabolic network. Entry genes (in black squares) and emerging new members of a pathway are colored by GO categories after enrichment analysis (Golorize/Cytoscape). Predicted interactions with members of the mitochondrial ETC Complex II, succinate dehydrogenase (SDH) are highlighted in the window. **D**, Gene interactions generated in GeneMANIA, between query genes SDH1-1, SDP6, GPDHc1, NOGC1 and FMO. Node functions related the genes to processes of energy and mitochondria metabolism. Functional links indicated co-expression (purple), co-localization (blue), predicted interaction (orange), and shared protein domains (brown), between the network components.

274 stress response and stomatal regulation (**Figure 4**). To better describe the system

275 transition during the stress treatments (O, P, OP), we performed a comparative

276 correlation analysis (**Steuer, 2006**) between regulation of glycerol, G3P shuttle

277 (*GPDHc1/SDP6*), mitochondria ETC (*SDH1*), and stomatal closure (*NOGC1/FMO*),
278 (**Figure 7A, 7B**), while GO network analyses (AraNet and GeneMANIA) provided
279 biological insights for possible functional relationships of these processes (**Figure 7C,**
280 **7D**). In AraNet, GO functional associations were predicted for genes of glycerol
281 metabolism which most strongly responded to the dynamics of the sequential treatment
282 (see **Figure 5**). Overall, the network was enriched in processes of fatty acid biosynthesis,
283 mitochondria metabolism (G3P shuttle), photosynthesis (chlorophyll biosynthesis,
284 sulfolipids, and photosystem stabilization), response to phosphate starvation, and
285 stomatal closure (**Table II**). New functional links between these processes highlighted
286 the connection between glycerol metabolism (particularly via the G3P shuttle; *GPDHc1*
287 and *SDP6*) and central energy metabolism - e.g. pentose phosphate shunt, NADPH
288 regeneration, glycolysis, ATP synthesis and mitochondrial ETC (**Figure 7C**). In AraNet,
289 *SDP6* linked to *SDH1-1* (**Figure 7C**), while GeneMANIA specifically predicted their
290 protein interaction and co-expression (**Figure 7D**). Consistently, we found that *SDH1-1*
291 and *SDP6* co-expressed most strongly during O₃ stress in O ($\rho = 0.97$, P -value = 0.005),
292 but also upon herbivory in P ($\rho = 0.95$, P -value = 0.01; **Figure 7A**). Up-regulation of
293 *SDH1-1* persisted in the sequential treatment OP (**Figure 7B**) but its co-expression with
294 *SDP6* was reduced ($\rho = 0.48$, P -value = 0.07; **Figure 7A**). Glycerol metabolism was
295 further associated to osmotic stress, stomatal closure and ABA response, via *SDP6*
296 interaction with flavin monooxygenases *NOGC1/FMO* and *SRE1/ABA2* (At1g52340;
297 **Nambara et al., 1998**) (**Figure 7C**). *NOGC1* and *FMO* were negatively correlated with
298 glycerol accumulation during O₃ stress in O (especially *FMO*, $\rho = -0.91$; P -value = 0.03)
299 but not in OP (**Figure 7A, 7B**). Moreover, *SDP6* interacted with water-glycerol protein

300 channels (*NIP* aquaglyceroporins, vacuole *BETA-TIP* and *GAMMA-TIP3*) and via
301 *NOGC1/FMO*, to the phosphate transporter *PHT2;1*(**Figure 7D**).

302

303 **Physiological Measurements of Photosynthesis and Gas Exchange**

304 Combined omics and network analysis highlighted the connection of glycerol and energy
305 metabolism with regulation of osmotic stress response and stomatal closure. In order to
306 assess the actual impact of O₃ and herbivory on *B. nigra*, we performed a second
307 experiment where we measured phenotypic and physiological parameters for plants
308 exposed to the stress treatments O, P and OP, and also for an additional long term O₃
309 stress of 16 days (OL) (**Figure 8A**). Although few individuals showed visible symptoms
310 of early senescence and chlorosis, chlorophyll content of the three youngest fully
311 expanded leaves (L5-L7) decreased by 9.5% after five days O₃ exposure (*P*-value <
312 0.05, n = 20) (**Figure 8B**). Herbivory alone did not directly affect chlorophyll levels, but
313 plants previously exposed to O₃ in the sequential treatment OP had 13.8 % lower
314 chlorophyll content compared to P (*P*-value < 0.05, n = 10) (**Figure 8B**). The deleterious
315 effect of O₃ was even more evident in the long term exposure (OL), where plants
316 revealed strong symptoms of senescence and chlorosis, particularly on the central fully
317 expanded leaves (L5-L7) (**Figure 8A**). Consistently, plants in OL showed a drastic 47.8%
318 decrease in chlorophyll compared to plants of the same age in C (*P*-value < 0.001, n =
319 10) (**Figure 8B**).

320 Five days of O₃ stress (O) to *B. nigra* plants also reduced photosynthetic activity,
321 decreased intracellular CO₂, and negatively affected stomatal conductance and leaf
322 transpiration (**Table III**). After 16 days exposure (OL), stomatal conductance decreased
323 even further, but intracellular CO₂ levels increased. 24 hours herbivory by *P. brassicae*

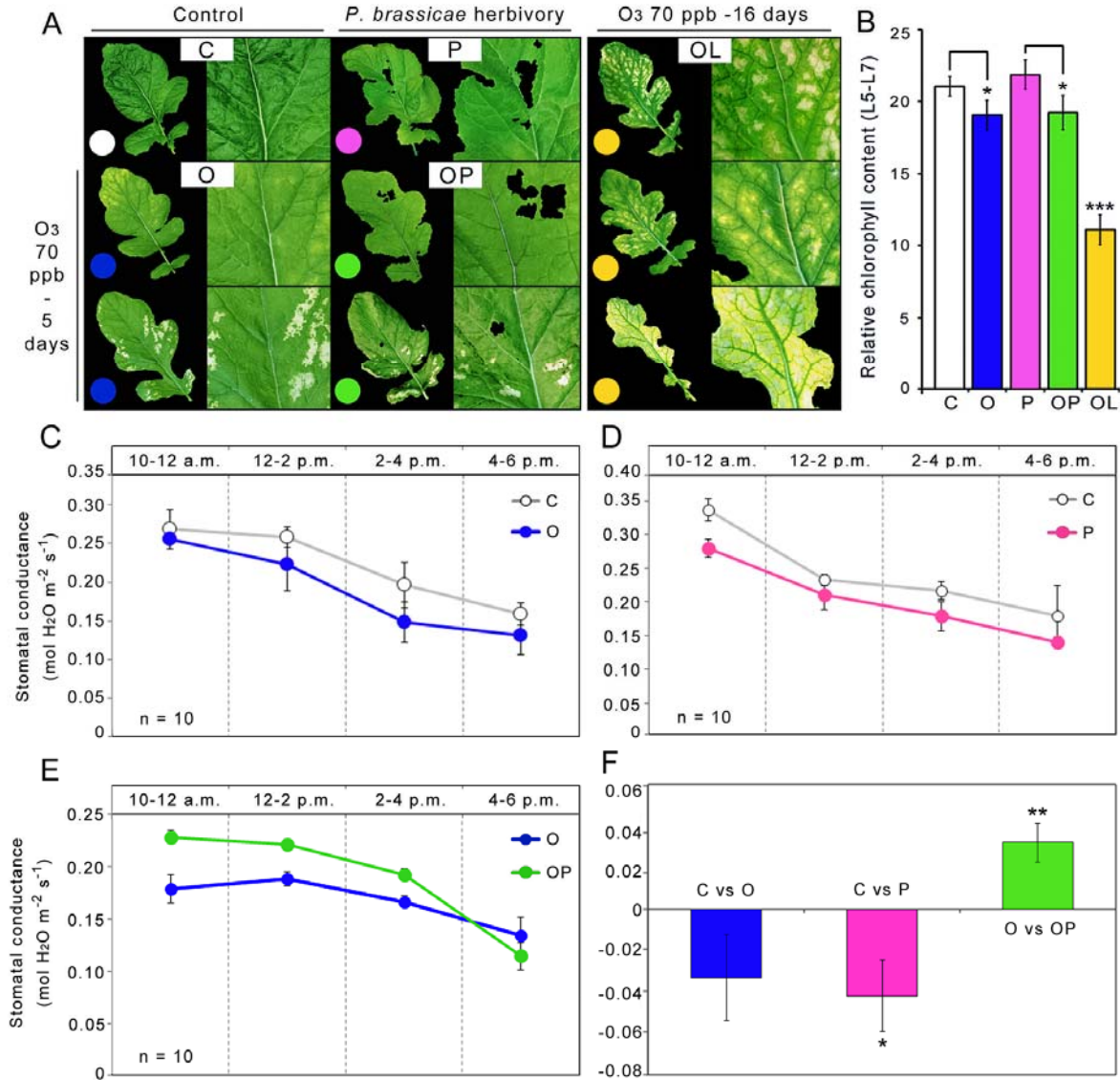


Figure 8 Physiological responses in *B. nigra*, under multiple O₃ and herbivory stress treatments. A, Leaf phenotypes of five weeks old *B. nigra* exposed to O₃ fumigation at 70 ppb for five days (O), herbivore-feeding with 30 first instar *P. brassicae* caterpillars for 24 hours (P), sequential stress of O₃ followed by herbivore-feeding (OP), long term exposure to O₃ at 70 ppb for 16 days (OL), or no treatment as controls (C). B, Relative chlorophyll content in leaf tissues was determined by optical absorbance at 653 nm for the three youngest fully expanded leaves (L5-L7). Student t-test shown between C and O (* P-value < 0.05; n = 20), P and OP (* P-value < 0.05; n = 10), C and OL (*** P-value < 0.001; n = 10). C-E, Stomatal conductance ($\mu\text{mol H}_2\text{O m}^{-2} \text{s}^{-1}$) of fully expanded leaves (L6) measured via steady-state porometry for three experimental setups during separate days (n=10 per treatment / day). F, Differences in stomatal conductance between the treatments and their controls were measured simultaneously. A one tailed t-tests evaluated if the mean difference between treatment responses was larger than zero: C versus O (P-value = 0.07); C versus P (P-value < 0.05; O versus OP (** P-value < 0.01). Bars = S.E.

324 (P) did not affect photosynthesis, but stomatal conductance and leaf transpiration
 325 decreased slightly compared to untreated controls (C). However, when herbivory
 326 followed (O) in the sequential treatment (OP), photosynthesis, stomatal conductance

327 and leaf transpiration were reactivated and thus expressed a reversed behaviour when
328 compared to the single stresses (**Table III**). As stomatal regulation follows the circadian
329 clock and decreases over the day, we further verified these conductance measurements
330 via steady-state porometry (**Figure 8C-D**). Similar to the previous results, conductance
331 decreased after single stress in O (P -value = 0.07; see also **Supplemental Figure 10**)
332 and in P (P -value = 0.02), whereas the sequential treatment OP induced stomatal re-
333 opening (P -value = 0.004) (**Figure 8F**).

334

335

336 **DISCUSSION**

337 Multiple stresses to plants may evoke unpredicted molecular responses with negative,
338 neutral or positive consequences for plant metabolism. We found molecular evidence of
339 photosystem and mitochondrial regulation in *B. nigra* in response to stress by O₃ and
340 sequential herbivory by *P. brassicae*. O₃ induced suppression of photosystem and
341 stomatal closure, but this response was re-directed to higher photosynthetic activity after
342 sequential addition of herbivores. Through omics multivariate and network analyses we
343 identified glycerol metabolism as a central driver of this shift. As predicted by the
344 combined omics -models, stomatal conductance and gas exchange were enhanced after
345 the sequential stress treatment, confirming a strategic change in *B. nigra* to emphasise
346 photosynthetic activity and energy metabolism. This response to sequential stresses
347 could not have been predicted from the individual stress responses, alone.

348

349 **Effects of O₃ stress on Photosynthesis and Stomatal Regulation**

350 O₃ stress negatively affects photosynthesis in plants (**Bagard et al., 2008; Salvatori et**
351 **al., 2015; Vainonen and Kangasjarvi, 2015**). It oxidizes thylakoid membranes in the
352 chloroplasts leading to symptoms like bleaching, chlorosis, and early leaf senescence
353 when chlorophyll is degraded (**Bergmann et al., 1999; Ranieri et al., 2001;**
354 **Goumenaki et al., 2010**). However, even before the symptoms appear, as
355 demonstrated in this study, the senescence process may be fully initiated with the down-
356 regulation of chlorophyll and light harvesting genes, and the induction of the
357 transcription factor *EIN3* that is involved leaf senescence (**Long and Naidu 2002;**
358 **Potuschak et al., 2003, Li et al., 2013**).

359 Besides photosystem suppression, chronic O₃ exposure above 40 ppb triggers a signal
360 cascade of reactive oxygen species (ROS) that causes stomatal closure to prevent O₃
361 from entering the leaf, but it also limits the CO₂ absorption (**Bergmann et al., 1999;**
362 **Castagna and Ranieri, 2009; Ranieri et al., 2001; Booker et al. 2009; Vahisalu et al.,**
363 **2010; Settele et al., 2014**). Our results confirmed a negative effect of O₃ on stomatal
364 conductance, leaf transpiration, and intracellular CO₂ levels, induced by stomatal closure
365 in *B. nigra*. After long-term exposure (70 ppb O₃ for 16 days) bleaching and chlorosis
366 also became obvious and the intracellular levels of CO₂ increased in agreement with
367 reduced assimilation rates and photosynthetic activity, which may further reinforce
368 stomatal closure (**Paoletti & Grulke 2005; Singh et al., 2009**).

369 O₃ stress also induced the expression of *MYB44*, which is thought to play a complex role
370 between abiotic and biotic responses such as drought and wounding (**Baldoni et al.,**
371 **2015**). During drought, overexpression of *MYB44* leads to enhanced tolerance through
372 regulation of stomatal closure in *Arabidopsis* mutants (**Jung et al., 2008**); however
373 *MYB44* also negatively regulates ABA responses (**Jaradat et al., 2013; Li et al., 2014**)
374 involved in stomatal closure, leaf senescence and ROS scavenging (**Persak and**
375 **Pitzschke, 2014**). In our study, expression of *MYB44* correlated positively with glycerol
376 levels, and negatively with *NOGC1*, an NO dependent guanylyl cyclase involved in
377 stomatal closure via Ca⁺⁺ signaling (**Mulaudzi et al., 2011; Joudoi et al., 2013**). In
378 addition, *MYB44* positively correlated ($\rho = 0.85$, P -value = 0.001) with a chloroplastic
379 lipid transfer protein *LTPc1* (At2g10940), which together with *LTPc2* (At2g45180) was
380 up-regulated during O₃ stress, but not herbivory (**Supplemental Figure S3,S4, and**
381 **Supplemental Table S3**). *LTPs* are known to be active in transfer of glycerolipids
382 between cell membranes - e.g. from chloroplasts to ER (**Xu et al., 2008**).

383 These results led us to suggest a coordinated regulation of *MYB44* and *NOGC1* in
384 response to O₃, which could serve as a feedback on ABA signaling and stomatal closure,
385 possibly connecting central energy metabolism and glycerolipid pathways involved in
386 osmotic stress responses.

387

388 **Importance of Glycerol and Energy Metabolism as Safety Valves**

389 Glycerol metabolism allows plants to adapt to a range of environmental stresses.
390 Spinach leaves for example accumulate triacylglycerol which is derived from membrane
391 galactolipids in response to O₃ fumigation (**Sakaki et al., 1990**). Regulation of
392 glycerolipid pathways is also induced in *Arabidopsis*, wheat, and saltbush in response to
393 temperature stress, which results in diacylglycerol trafficking from ER to chloroplast (**Li**
394 **et al., 2015**). In *Arabidopsis*, heat, salt, and drought also induce triacylglycerol
395 accumulation in the cytosol, as an adaptation that enables structural remodeling of
396 membrane lipids (**Mueller et al., 2015**). In our study, the combination of photosystem
397 suppression and decrease of chlorophyll content suggests that glycerol may originate
398 from degradation of chloroplasts and glycolipid membranes in response to O₃ stress.
399 Increased glycerol levels were further correlated with regulation of genes involved in
400 stomatal closure and osmotic stress responses (*MYB44*, *NOGC1*, and *FMO*). Glycerol
401 has osmolyte properties, and its accumulation in mutants that lack glycerol kinase
402 enhances *Arabidopsis* resistance to dehydration stress (**Eastmond, 2004**).
403 GO network analyses further emphasized the presence of a connection between
404 osmotic stress response, glycerol metabolism, and central energy processes of
405 chloroplasts and mitochondria.

406 Without CO₂ to assimilate the photons harvested from photosynthesis, plants suppress
407 their photosystem and activate non-photochemical quenching to protect cellular
408 structures against excess excitation energy (**Niyogi, 2000; Murata et al., 2007**).

409 Mitochondria also act as sinks for excess electrons that follow oxidative stress, and
410 oxidize reducing equivalents via respiration (**Hoefnagel et al., 1998; Niyogi, 2000;**
411 **Scheibe et al., 2005; Noctor et al., 2007; Nunes-Nesi et al., 2008**).

412 In our study, increased activity of the mitochondrial manganese superoxide dismutase
413 *MSD1* (**Tsang et al., 1991; Martin et al., 2013**) (**Figure 5D**), suggests that mitochondria
414 also play a role in the oxidative stress response against O₃. This was further supported
415 by the increased activity of the mitochondrial succinate dehydrogenase *SDH1-1* and of
416 the glycerol-3P shuttle (*GPDHc1/SDP6*). In the mitochondrial ETC, *SDH1-1* acts as
417 binding site for coenzyme Q in Complex II (**Huang et al., 2013**), while the G3P shuttle is
418 pivotal in supplying the ETC with redox energy derived from NADH (**Shen et al., 2006;**
419 **McKenna et al., 2006; Berg et al., 2012; Mráček et al., 2013**). Curiously, we found that
420 the phosphate response genes (*RNS1, PT2*) were up-regulated, while our GO- network
421 analyses linked glycerolipid metabolism to phosphate starvation (*SQD2, DGD1*).

422 Phosphate starvation symptoms are similar to those of O₃ stress including down-
423 regulation of photosystem, low CO₂ assimilation, photo-oxidation of membrane lipids
424 (**Hernández and Munné-Bosch, 2015**), transfer of digalactosyldiacylglycerol from
425 chloroplast to mitochondria (**Jouhet et al., 2004**), and membrane lipid remodeling in
426 *Arabidopsis* with down-regulation of *SQD2* (**Jost et al., 2015**). Overall, cumulative
427 regulation of glycerol metabolism may reflect a flux reconfiguration to sustain
428 mitochondria activity, resulting in increased glycerol pools as an intermediate metabolite

429 in the pathway (**Kleijn et al., 2007; Morandini, 2013; Gomes de Oliveira Dal'Molin et**
430 **al., 2015**).

431

432 **Sequential Herbivory after O₃ Stress Induces Abiotic and Biotic Crosstalk**

433 Herbivory by *P. brassicae* induced down-regulation of photosystem and reduced carbon
434 assimilation rates, although with a less severe impact compared to O₃ stress. Chewing
435 herbivores systemically reduce photosynthetic activity in damaged leaves and in
436 neighboring tissues (**Zangerl 2002; Bilgin et al., 2010; Halitschke et al., 2011**),
437 whereas JA signaling and lipoxygenases (*LOXs*) directly affect photosystem and ETC
438 activity in chloroplasts (**Nabity et al., 2012; Havko et al., 2016**). The underlying
439 mechanisms that suppress photosynthesis in favor of induced-defense responses are
440 not fully understood, but a trade-off between allocation of resources to growth and
441 defense appear to determine how plants rearrange their metabolism and redirect
442 primary resources towards the production of specialized defensive compounds
443 (**Schwachtje and Baldwin, 2008; Tang et al., 2009; Meldau et al., 2012**). Upon
444 herbivory, *B. nigra* induced a slight stomatal closure, although we did not observe a
445 distinct up-regulation of *MYB44* expected after biotic stress and wounding (**Jung et al.,**
446 **2010, Shim et al., 2013; Persak and Pitzschke, 2013**). While *MYB44* was up-regulated
447 and stomata closed in the O₃ stressed plants, addition of herbivores in the sequential
448 stress caused stomata to reopen. Thus, the resulting phenotype resembled the one
449 observed after herbivore damage alone, with a relatively low stomatal conductance.
450 Sequential herbivory positively induced the expression of *MYC2* (JA-signaling) and
451 negatively affected *EIN3* (ET-signaling) previously induced by O₃. *MYC2* and *EIN3* are
452 key integrators of plant abiotic and biotic stress responses (**Abe et al., 2003; Anderson,**

453 **2004; Fujita et al., 2006; Dombrecht et al., 2007; Atkinson et al., 2013**). In a mutual
454 antagonistic interaction, JA-activated *MYC2* is known to repress transcription of
455 *EIN3/EIL1*, while induction of *EIN3/EIL1* reciprocally represses *MYC2* and JA responses
456 **(Song et al., 2014; Zhang et al., 2014; Song et al., 2015; Kim et al., 2015)**.
457 Similarly, *ERF2*, which is involved in ET-signaling **(Fujimoto et al., 2000)** and in positive
458 regulation of JA-responses **(McGrath et al., 2005; Pré et al., 2008)** was down-regulated
459 after single O₃ stress, but it was induced during single and sequential herbivory. This
460 asymmetric regulation of ABA and JA/ET pathways, in connection with stomata behavior,
461 suggests a specific cross-talk that balanced the metabolic responses to O₃ and
462 herbivory in the sequential stress situation.

463

464 **O₃ and Herbivory Affect Central Metabolism in Opposite Ways**

465 In a previous study, we showed that interaction between O₃ stress and herbivory in *B.*
466 *nigra* induced changes in the plant secondary metabolism (glucosinolates and
467 phenolics), and while O₃ fumigation at 120 ppb promoted feeding damage by *P.*
468 *brassicae*, the performance and fitness of the caterpillars was characterized by delayed
469 development and lighter pupae **(Khaling et al., 2015)**.

470 Here we show that central (primary) metabolism also plays a pivotal role in the plants
471 response to concurrent abiotic and biotic stressors. Both transcriptomics and
472 metabolomics indicated an alteration of the carbon and nitrogen metabolism in response
473 to O₃ stress. Pools of central metabolites increased, while the activity of many genes
474 involved in carbohydrate metabolism and cell-wall biosynthesis was reduced, including
475 down-regulation of *F2KP* (fructose-2,6 bisphosphatase/phosphofructokinase), the

476 central regulator of glycolysis and gluconeogenesis (**Draborg et al., 2001; Nielsen et al.,**
477 **2004; McCormick and Kruger, 2015**)(**Figure 5B**). Up-regulation of genes involved in
478 amino acid metabolism further supports an increased flux towards mitochondrial
479 metabolism and nitrogen mobilization, resembling patterns of senescence (**Bouché et**
480 **al., 2003; Li et al., 2006; Breeze et al., 2011; Debouba et al., 2013 Watanabe et al.,**
481 **2013**). Similar effects of O₃ stress on the central metabolism were reported in other
482 studies in which routes of detoxification and redox balance (e.g. aldehyde
483 dehydrogenase *ALDH*, chloroplastic *SOD* activity, NADH regeneration) were coupled to
484 stomatal closure, decrease in photosynthesis, and increase in mitochondrial respiration
485 (**Dizengremel et al., 2009; Yendrek et al., 2015**). However, once herbivory was applied
486 as a second stress, all these initial effects of O₃ were reversed, resulting in decreased
487 levels of sugars and amino acids and a reconfiguration of gene expression, including
488 down-regulation of the amino acid transporter *AAP2*, which promotes nitrogen
489 accumulation in siliques and seed development in *Arabidopsis* (**Hirner et al., 1998;**
490 **Ortiz-Lopez et al., 2000**).

491 Interestingly, a common response to both O₃ and herbivory was the increase in the
492 central metabolite GABA. In mitochondria, the GABA shunt delivers additional succinate
493 and NADH to the ETC, and provides an alternative route to the amino acid metabolism
494 (**Bouché et al., 2003**). During abiotic and biotic stresses, GABA concentrations can
495 rapidly spike, but its function in plant response is still under investigation (**Bouché and**
496 **Fromm, 2004; Fait et al., 2008**). Studies show that GABA is involved in stress signaling
497 processes, from leaf senescence (**Ansari et al., 2005**) to plant communication with
498 insects and microorganisms (**Shelp et al., 2006; Michaeli and Fromm, 2015**). Under

499 conditions of oxidative stress and inhibited photosynthesis, GABA participates in
500 scavenging ROS in support of normal growth and stress tolerance (**Bouché et al., 2003;**
501 **Dizengremel et al., 2012**). GABA has also been proposed to regulate the carbon and
502 amino acid metabolism of plants through interaction with GABA/glutamate receptors
503 (GLR) in concert with differential regulation of the ABA/ET signaling pathways (**Lancien**
504 **and Roberts, 2006; Forde and Lea, 2007**). Accordingly, in our study, increased levels
505 of GABA may play a role in maintenance of central metabolism, oxidative stress
506 response, and/or regulation of stomatal closure, possibly via GLR and Ca⁺⁺ signaling.

507
508 In conclusion, we propose the presence of a tolerance mechanism in *B. nigra* (**Figure 9**)
509 where glycerol and central energy metabolism play a central role in the adaptation to the
510 sequential stress by O₃ and herbivory, and which enables *B. nigra* to prioritize demands
511 of stomatal osmoregulation and oxidative stress. The suppression of photosynthesis and
512 regulation of glycerol and mitochondrial metabolism during O₃ stress possibly dissipate
513 excess energy to avoid formation of oxidative radicals (**Hoefnagel et al., 1998**),
514 combining fast NAD⁺ recycling with maintenance of central metabolism and growth
515 (**Dizengremel et al., 2008, and 2012**). This hypothesis is supported by previous studies
516 on the physiological functions of glycerol metabolism in NADH/NAD⁺ homeostasis
517 (**Shen et al., 2006; Quettier et al., 2008**), osmotic stress response (**Biela et al., 1999;**
518 **Eastmond, 2004; Chen et al., 2011; Geijer et al., 2012**), and plant development (**Hu et**
519 **al., 2014**). These pathways were redirected in the sequential treatment, during which
520 glycerolipid resources may have been reallocated towards JA signaling and induction of
521 defense against herbivores (**Turner et al., 2002; Kachroo et al., 2004; Havko et al.,**
522 **2016**). Alternatively, these reversed effects may also represent a manipulation of the

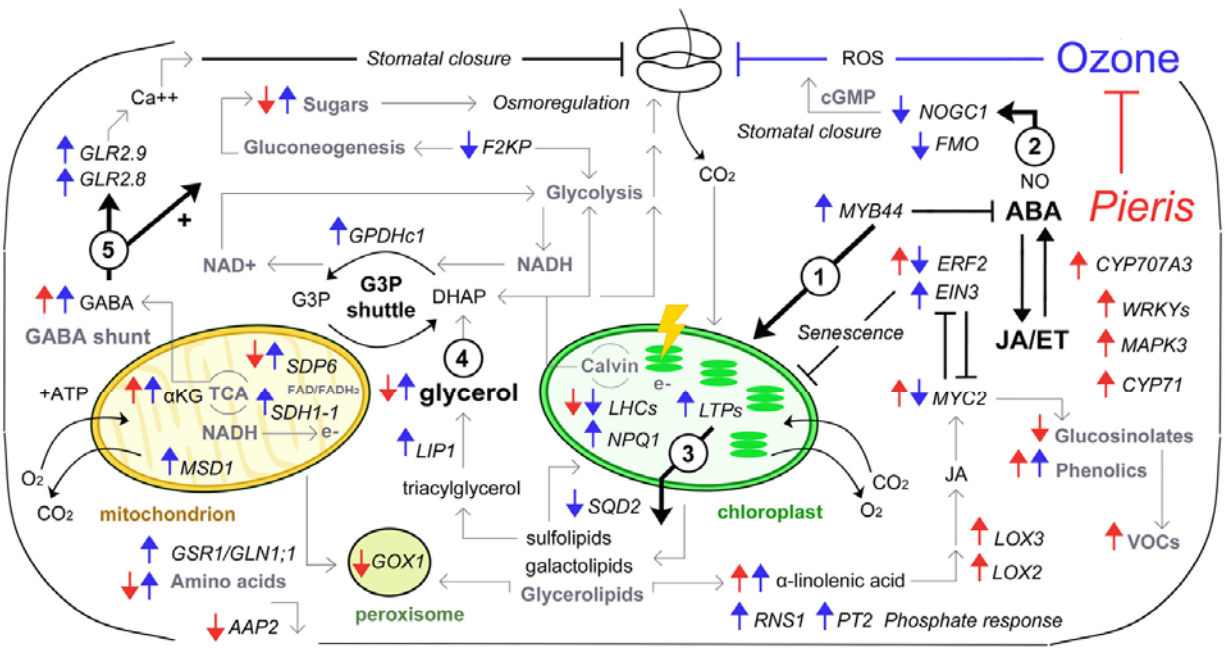


Figure 9 Summary of omics and physiological responses in *B. nigra* during sequential O₃ and herbivory stress treatments. The model links metabolome and transcriptome fluctuations to physiological responses of photosystem, CO₂ assimilation and stomatal opening. Stress adaptation mechanisms are proposed (1-5). Blue: O₃ fumigation (5 days at 70ppb, 16h/day). Red: O₃ followed by *P. brassicae* (24 h, 30 1st instar caterpillars). Upward arrows indicate up-regulation (genes) or increase (metabolites) and downward arrows the opposite. 1-2, Ozone induces abiotic stress responses of senescence (EIN3, ERF2) and stomatal closure (MYB44) with feedback on NO-guanylate cyclase/flavin monooxygenases (NOGC1, FMO). ABA and JA/ET crosstalk integrates responses between O₃ and sequential herbivory (MYC2, ERF2), with opposite effect on stomatal closure. 3-4, Photosystem suppression (LHCs) and non-photochemical quenching (NPQ1) in response to O₃ are linked to regulation of glycerolipid metabolism (LPTs, LIP1, SQA2). Glycerol derived from degraded chloroplast membranes enters the G3P shuttle (GPDHc1/SDP6) to sustain NAD⁺ recycle and mitochondrial activity (SDH1-1, MSD1, GABA) as anti-oxidative stress mechanism. A possible role of glycerol and sugars as osmolytes is also suggested. Sequential herbivory restores the glycerolipid pathway for alternative source-sink priorities - e.g. JA responses (LOXs/MYC2). 5, GABA plays multiple roles in plant stress adaptation, regulating Ca⁺⁺ homeostasis, carbon-nitrogen metabolism, leaf senescence, ROS scavenging, and signaling of plant-insect interactions.

523 host metabolism by the herbivore (**Karban and Agrawal, 2002**), which can interfere with
 524 plant defense and water-stress response genes (**Reymond et al., 2000; Consoles et al.,**
 525 **2012**).

526

527 MATERIALS AND METHODS

528 Plants

529 Seeds from black mustard plants (*Brassica nigra*) obtained from the Laboratory of
530 Entomology of Wageningen University (The Netherlands), were collected from a natural
531 population growing along the Rhine river in Wageningen. The seeds were planted
532 individually in plastic pots (9x9x9.5cm) filled with a 3:1:1 mix of peat, potting compost,
533 and sand. They were grown under greenhouse conditions at the University of Eastern
534 Finland, Kuopio, (FIN). The plants were watered intermittently with sprinklers for five
535 hours every day without chemical control for pests or diseases. The seedlings were
536 fertilized twice per week with 0.1% 5-Superex, (N: P: K 19:5:20) Kekkilä, Finland. When
537 the plants were four weeks old and had developed approximately 7 leaves, they were
538 taken to growth chambers (Weiss Bio 1300; Weiss Umwelttechnik GmbH, Preskirchen-
539 Lindenstruth, Germany) and subjected to the different treatments for 6 days.

540

541 Treatments

542 Plants were subjected to one of four treatments: exposure to ambient air with and
543 without feeding by *Pieris brassicae* caterpillars (C and P), and O₃ fumigation with and
544 without subsequent feeding by *P. brassicae* caterpillars (O and OP). The experiment
545 was repeated five times (biological replicates) with each replicate including three plants
546 per treatment. Two extra replicates were produced for the evaluation of gene expression
547 after exposure to ambient air and *P. brassicae* feeding (seven replicates in total).

548

549

550 **O₃ Fumigation**

551 The plants (12 in total, three per treatment) were moved to plant growth chambers. The
552 chambers had been modified so that each had an independently controlled O₃
553 concentration. High O₃ chambers were set to 70 ppb from 4 AM to 8 PM and maintained
554 at a basal O₃ concentration of 30 ppb for the remaining hours each day. This was done
555 to imitate natural diurnal variation in O₃ concentration. In ambient chambers, the O₃
556 concentration fluctuated between 15 and 20 ppb. Chambers were maintained at a
557 temperature of 23 ± 3°C, relative humidity of 60% during the day and 80% at night and a
558 photoperiod of L16h:D8h with a light intensity of 300 μmol m⁻²s⁻¹. The plants were
559 watered daily. The above conditions were maintained for five days, after which the
560 plants subjected to herbivore feeding were infested for a period of 24 hours.

561

562 **Herbivore Feeding**

563 The large cabbage white butterfly, *Pieris brassicae* (Lepidoptera: Pieridae), was
564 obtained from stocks at the Laboratory of Entomology, Wageningen University and
565 reared on Brussels sprouts plants (*Brassica oleracea* var. *gemmifera* L. cultivar Brilliant)
566 at the University of Eastern Finland under greenhouse conditions. Prior to experiments,
567 *P. brassicae* adults were presented with *B. nigra* plants for oviposition and first instar
568 caterpillars were collected soon after hatching in a climate controlled insect rearing room
569 with a temperature of 25 ± 2°C, photoperiod of 16 h light / 8 h darkness, light intensity of
570 300 μmoles m⁻²s⁻¹ and RH of ca. 60%. For the herbivore treatment, a total of 30 first
571 instar *P. brassicae* caterpillars were mounted on the three highest fully expanded leaves
572 of each plant (ten caterpillars per leaf) and left to feed for 24 hours. After 24 hours (day

573 six), VOCs were collected and plant samples were harvested for metabolomics and
574 transcriptomics analyses.

575

576 **Physiological Measurements of Photosystem and Gas Exchange**

577 Chlorophyll relative content in leaf tissues was determined by optical absorbance at 653
578 nm (CCM-200 plus; Opti-science®) for the three youngest fully expanded leaves (L5-L7).
579 Photosynthetic and gas exchange parameters – i.e. carbon assimilation rate ($\mu\text{mol CO}_2$
580 $\text{m}^{-2} \text{s}^{-1}$), intracellular CO_2 , stomatal conductance and leaf transpiration ($\mu\text{mol H}_2\text{O m}^{-2} \text{s}^{-1}$)
581 – were measured for a period of ca. 1 hour, on one fully expanded leaf (L6) per plant (n
582 = 10) using a LI-COR® gas analyzer (LI-6400). The leaf chamber parameters were set
583 to mimic the ambient growth conditions, with block temperature at 24°C, RH at 60%,
584 CO_2 at 400 $\mu\text{L L}^{-1}$, and saturating light at 1000 $\mu\text{mol m}^{-2} \text{s}^{-1}$. In addition, leaf (L6)
585 stomatal conductance was determined via steady-state porometry (SC-1, Decagon
586 Devices®), which measured the actual water vapor flux ($\mu\text{mol H}_2\text{O m}^{-2} \text{s}^{-1}$) from the leaf
587 through the stomata and out to the environment.

588

589 **Sampling for Metabolomics and Transcriptomics**

590 At the time of sampling, the plants were four weeks + six days old. Counting from the
591 apex, the three youngest fully expanded leaves (L5-L7) of each of the three plants
592 (altogether 9 leaves from 3 plants per treatment) were cut at the petiole with a sharp
593 knife and pooled together. The detached leaves were then immediately wrapped in tin
594 foil and flash frozen in liquid nitrogen. The leaves were stored at -80°C and later ground
595 with mortar and pestle together with liquid nitrogen into a fine powder. Equal amounts of
596 powder from each sample were sent express on dry ice to the laboratories in Umeå, (SE)

597 and Lausanne, (CH), for metabolomics and transcriptomics analyses, respectively.
598 Exactly the same samples were thus shared between the laboratories.

599

600 **Metabolomics Analyses**

601 All metabolomics analyses were performed at Umeå Plant Science Center - Swedish
602 Metabolomics Center (UPSC-SMC), Umeå (Sweden). For the preparation of LC-MS and
603 GC-MS leaf tissue analysis, 10-12 mg of frozen sample were extracted using 1 ml of
604 cold chloroform:methanol:H₂O (20:60:20), containing 7.5 ng/μl of labeled salicylic acid-
605 D₄ (m/z [M-H]⁻ 141.046) as internal standard (IS). A 3 mm tungsten carbide bead was
606 added in each vial, and samples were agitated for 3 min at 30 Hz in a MM 301 Vibration
607 Mill (Retsch GmbH and Co. KG, Haan, Germany). In order to separate the mixture from
608 tissue debris and avoid contamination, extracts were centrifuged at 20.800 × g for 10
609 min at 4°C. 200 μl of the supernatant was evaporated to dryness using a SpeedVac™.
610 For GC-MS analysis samples were derivatized using 30 μl of methoxyamine (15 ug/μL in
611 pyridine) and shaken for 10 min and thereafter letting it react for 16 hours at 25°C.
612 Silylation was achieved using 30 μl of MSTFA reacting for 1 hour at 25°C. Finally,
613 samples were diluted with 30 μl of heptane containing 15ng/μl of methyl stearate
614 (internal standard), and injected into the system. For LC-MS analysis, dried samples
615 were then re-dissolved in 10 μl cold methanol and diluted with 10 μl cold water, and
616 injected into the system.

617

618 **GC-MS**

619 One μL of the derivatized sample was injected splitless by a CTC Combi Pal
620 autosampler (CTC Analytics AG, Switzerland) into an Agilent 6890 gas chromatograph

621 equipped with a 10 m x 0.18 mm i.d. fused silica capillary column with a chemically
622 bonded 0.18 μm DB 5-MS UI stationary phase (J&W Scientific). The injector
623 temperature was 270 $^{\circ}\text{C}$, the purge flow rate was set to 20 ml min⁻¹ and the purge
624 turned on after 60 s. The gas flow rate through the column was 1 ml min⁻¹, the column
625 temperature held at 70 $^{\circ}\text{C}$ for 2 minutes, then increased by 40 $^{\circ}\text{C}$ min⁻¹ to 320 $^{\circ}\text{C}$, and
626 held for 2 min. The column effluent was introduced into the ion source of a Pegasus III
627 time-of-flight mass spectrometer, GC/TOFMS (Leco Corp., St Joseph, MI, USA). The
628 transfer line and the ion source temperatures were set to 250 $^{\circ}\text{C}$ and 200 $^{\circ}\text{C}$,
629 respectively. Ions were generated by a 70 eV electron beam at an ionization current of
630 2.0 mA, and 30 spectra s⁻¹ were recorded in the mass range 50 - 800 m/z. The
631 acceleration voltage was turned on after a solvent delay of 150 s. The detector voltage
632 was set to 1700 V.

633

634 **LC-MS**

635 For analysis of secondary metabolites, samples were analyzed by ultra-high
636 performance liquid chromatography -electrospray ionization/ time of flight mass
637 spectrometry (UHPLC-ESI/TOF-MS, Waters, Milford, MA USA). The Acquity™ system
638 was equipped with a 2.1×100 mm, 1.7 μm C18 UPLC™ column (reversed phase column
639 /non-polar stationary phase) held at 40 $^{\circ}\text{C}$. The LC system was coupled to an LCT
640 Premier TOFMS. 2 μl of each sample were injected and separated throughout the
641 mobile phase containing a mix of solvents A (H₂O + 0.1% formic acid) and B
642 (acetonitrile + 0.1% formic acid). The elution gradient between over time of solvent B
643 over A was: 0–4 min 1–20%, 4–6 min 20–40%, 6–9 min 40–95%, 9–13.5 min 95%. The
644 total running time for each sample was 19 min, with a flow rate of 500 $\mu\text{l}/\text{min}$. The source

645 temperature was 120°C, cone gas flow 10 L/h, desolvation temperature 320°C,
646 nebulization gas flow 600 L/h, and the capillary and cone voltages were set at 2.5 kV
647 (negative ionization mode) and 35 V , respectively. Data were acquired in dynamic
648 range enhancement (DRE) mode every 0.1 s, with a 0.01 s inter-scan delay. The lock
649 mass compound for accurate mass measurements (leucine enkephalin) was infused
650 directly at 400 pg/μl in 50:50 acetonitrile:H₂O at 20 μl/min. The normal lock mass in
651 DRE mode was the negative ¹³C ion of leucine enkephalin (m/z 555.265), and the
652 extended lock mass was the normal negative ion (m/z 554.262). Mass spectra were
653 acquired in centroid mode with m/z range 100–1000 and data threshold value set to 3.
654

655 **Orbitrap MSMS**

656 In order to verify the data acquired by the UHPLC-ESI/TOF-MS, samples were re-
657 analyzed for determination of selected peaks of interest by UHPLC-MS-MS using linear
658 ion trap (LTQ-Orbitrap). Separation was performed on a Thermo Accela LC system,
659 equipped with a column oven (held at 40°C) and a Hypersil C18 GOLD™ column
660 (2.1×50 mm, 1.9 μm; mobile phase as for the UHPLC-ESI/TOFMS) and analyzed by
661 tandem mass spectrometry using a LTQ/Orbitrap mass spectrometer (Thermo Fisher
662 Scientific, Bremen, Germany). External mass calibration was performed according to the
663 manufacturer's guidelines.

664

665 **Data Processing and Identification**

666 GC-MS was operated with the LECO ChromaTOF® software (optimized for Pegasus HT;
667 Leco Corp., St Joseph, MI, USA). Retention time indexes (RIs) were calculated relative
668 to an alkane series C8-C40. From the raw data, feature extraction and peak integration

669 were all performed with Matlab®, combining target analysis (a predefined list of retention
670 time windows and m/z values) and automated peak deconvolution. Compounds were
671 identified comparing RIs and mass spectra to UPSC-SMC in-house database, and to the
672 public Golm Metabolome Database of the Max Planck Institute (GMD-MPI). For the
673 comparison with the GMD, RIs measured on the 5%-phenyl-95%-dimethylpolysiloxane
674 capillary column - VAR5 (GMD) were transferred to the DB-5 (10m) system of UPSC-
675 SMC (Strehmel et al., 2008; Hummel et al., 2010). Samples were normalized on the
676 UVN scores of integrated areas for IS (methyl stearate and salicylic acid-D4).
677 The UHPLC-ESI/TOFMS instruments were operated with MassLynx™ v. 4.1 software
678 (Waters, Milford, MA, USA). Compounds from LC-MS analysis were compared to
679 standards of glucosinolates (sinigrin, glucobrassicin, gluconapin, glucotropaeolin,
680 gluconasturtiin, sinalbin - PhytoPlan, Diehm & Neuberger GmbH, Heidelberg, Germany),
681 METLIN mass spectra depository, and additional literature references for glucosinolates
682 (Clarke, 2010) and for flavonol glucosides and hydroxycinnamic acid derivatives (Lin et
683 al., 2011). Tandem mass data analysis by Orbitrap was used to compare the MSn
684 profiles and further confirm the identifications. Raw data were processed using Sieve®
685 and Matlab® software for peak alignment and integration. The peak areas were
686 normalized against that of the labeled internal standard of salicylic acid-D4 (m/z [M-H-]
687 141.046).

688

689 **VOCs Collection and Analyses**

690 All VOC collection and analyses were performed at the University of Eastern Finland,
691 Kuopio (Finland). The plants were first enclosed in glass jars. Filtered air was fed into
692 the glass jars at a rate of 250 ml min⁻¹ and pulled out at a rate of 200 ml min⁻¹ through

693 stainless steel tubes filled with Tenax TA and Carboxen 100 adsorbents (150 mg each;
694 mesh 60/80; Markes International, Llantrisant, RCT, UK). The samples were collected
695 for 60 minutes. The plant volatiles were analyzed by gas chromatography–mass
696 spectrometry (GC–MS; Agilent 7890A GC and 5975C VL MSD; New York, USA).
697 Trapped compounds were desorbed with an automated thermal desorber (TD-100;
698 Markes International Ltd, Llantrisant, UK) at 250 °C for 10 min, cryofocused at –10 °C,
699 and then injected in a split mode onto an HP-5 capillary column (50 m×0.2 mm; film
700 thickness 0.33 µm) with helium as a carrier gas. The oven temperature program was
701 held at 40 °C for 1 min, then raised to 210 °C at a rate of 5 °C min⁻¹ and then further to
702 250 °C at 20 °C min⁻¹. The column flow was maintained at a rate of 1.2 ml min⁻¹. The
703 compounds were identified by comparing the mass spectrum of an individual compound
704 to the spectra of compounds in an external authentic standard and to compounds in the
705 Wiley Library. Relative emissions were measured by peak integration (absolute rates
706 expressed as nmol m⁻²hr⁻¹ are reported in the **Supplemental Dataset S2**.

707

708 **Transcriptomic Analyses**

709 Transcriptomics analyses were performed at University of Lausanne, Lausanne
710 (Switzerland). *Brassica nigra* leaves (3-6 g) were ground in liquid N₂ and total RNA was
711 extracted, reverse-transcribed, and processed according to a previously published
712 procedure (**Bodenhausen and Reymond, 2007**). Labeled probes were hybridized onto
713 CATMA v4 microarrays containing 32,998 *A. thaliana* gene-specific tags and gene family
714 tags (**Sclep et al., 2007**). Hybridization and scanning have been described previously
715 (**Reymond et al., 2004**). Data analysis was carried out using an interface developed at
716 the University of Lausanne (Gene Expression Data Analysis Interface) (**Liechti et al.,**

717 **2010**). Differentially expressed genes were identified by fitting a linear model for each
718 gene and evaluating the fold change and moderated t statistic *P*-values (**Smyth, 2004**).
719 To address the issue of multiple comparisons we used the false discovery rate method
720 of **Storey and Tibshirani** and computed a *q* value (**2003**). Because we employed
721 Arabidopsis whole-genome microarrays to probe expression of *Brassica nigra* genes,
722 the number of genes that produced hybridization signals was clearly low and overall
723 hybridization signal intensity was also weaker than with Arabidopsis samples. Hence, we
724 noticed that high FDR values are estimated when the number of induced genes is
725 relatively small. However, by comparing gene expression between experiments, genes
726 with small *P*-values in response to one treatment often had a small *P*-value in another
727 treatment. Thus interexperiment comparison adds to data interpretation, and FDR
728 calculations might be too conservative in some cases. For data analysis, we thus used
729 an unadjusted *P*-value of 0.05. FDR values are indicated in **Supplemental Dataset S1**.

730

731 **Statistical Analyses**

732 Matrixes for gene expression and metabolites were created in Excel®. All steps of basic
733 statistic (i.e. Pearson's correlation, Student t-test, ANOVA and post-hoc Tuckey test)
734 were performed with Excel and with Minitab 17 Statistical Software® (2010) State
735 College, PA: Minitab, Inc. (www.minitab.com). Other more specific analyses have been
736 performed with the open-source software R (<https://www.r-project.org/>) and RStudio
737 (<https://www.rstudio.com/>) or with other software as mentioned below.

738

739

740

741 **Multivariate Analyses**

742 Gene expression and metabolite profiles were subjected to multivariate analysis using
743 SIMCA® 14 software package (Umetrics, Umeå, Sweden). Supervised regression
744 models such as partial least square (PLS) an orthogonal projection of latent structures
745 (OPLS) discriminant analysis (DA) were used to investigate the variation in X-variables
746 (gene or metabolites) which was modeled for the Y-explanatory variables, corresponding
747 to O₃ and *P. brassicae* treatments. The cumulative (c) variation in X and in Y explained
748 by the models is reported by the terms R²X(c) and R²Y(c) respectively. Models were fit
749 to the minimum number of latent variables (LVs) corresponding to the highest value of
750 predicted variation - Q²(c). Selection of important variables was based on the Variable
751 Importance for Projection (VIP) score, considered significant if above the threshold of
752 1.00.

753

754 **Gene Expression Data Evaluation and Pathway Analyses**

755 Gene selection for student t-test cut-off of *P*-value ≤ 0.05 was executed in Excel. The
756 open-source software R (and RStudio) was used to create heat-maps, hierarchical
757 clustering, and correlation of gene expression profiles using the CRAN library packages
758 and functions *heatmap* (gplots), *hclust* and *corrgram* respectively. More specifically,
759 gene expression values for each sample (up- or down- regulation) were represented
760 graphically using the *heatmap* function, while rows (genes) and columns (samples) of
761 the matrix were reorder in dendograms following hierarchical clustering. The default
762 function *hclust* was used with its method of complete linkage which agglomerates
763 clusters computing the largest distance between any object in one cluster and the other
764 objects in the other clusters. Similarity between each sample group was further tested

765 using the *corrgram* function (default method Pearsons's correlation). Thus, a correlation
766 matrix was produced as a graphical display (i.e. the correlogram) with cells colored
767 according to the respective correlation coefficient (ρ) for each of the paired sample
768 comparison.

769 Gene ontology (GO) enrichment analysis of the gene clusters was performed with the
770 web-based tool Functional Classification SuperViewer of the University of Toronto
771 (Canada) (http://bar.utoronto.ca/ntools/cgi-bin/ntools_classification_superviewer.cgi)
772 where GO categories for genes in a given cluster are normalized for the frequency in
773 Arabidopsis, while bootstraps and standard deviation provide confidence intervals for the
774 accuracy of the output (**Provar and Zhu, 2003**). *P*-values of the hypergeometric
775 distribution were used to select the significant functional classes. Only enrichments with
776 significant *P*-values ≤ 0.05 were considered and reported in the graph. The MapMan
777 tool (**Thimm et al., 2004**); <http://mapman.gabipd.org/web/guest>) was used for
778 visualization of the gene expression dataset in the context of metabolic pathways or
779 other processes represented in modules ("bins"), and in order to build the Venn
780 diagrams for up- and down- regulated genes. Beside MapMan, other resources used for
781 pathway analysis and interpretation of "omics" data included the free databases KaPPA
782 View4 (**Tokimatsu et al., 2005; Sakurai et al., 2011**); <http://kpv.kazusa.or.jp/>) and
783 Kyoto Encyclopedia of Genes and Genomes (KEGG) database (**Kanehisa and Goto,**
784 **2000**; <http://www.genome.jp/kegg/>). Gene sub-cellular localizations and expressions
785 were searched with the ePlant server of the University of Toronto
786 (Canada)(<https://bar.utoronto.ca/eplant/>).

787

788

789

790 **Integrative Omics Network Analyses**

791 The open source platform Cytoscape (version 3.2.1) was used for visualization and
792 analysis of the omics networks. The correlation matrix between genes and metabolites
793 was computed into a similarity network using the *ExpressionCorrelation* app
794 (<http://apps.cytoscape.org/apps/expressioncorrelation>). The network was built setting the
795 edge (links) parameters to Pearson's coefficient $\rho \geq 0.85$ for both positive and negative
796 correlations. For network visualization, the graphic layout was set to (yFile) "organic".
797 Network topological features were evaluated with *Network Analyzer* (Max Planck Institut
798 Informatik; **Assenov et al., 2008**). For comparative correlation analysis, the network
799 between glycerol and the five genes components – *GPDHc1* (At2g41540), *SDP6*
800 (At3g10370), *NOGC1* (At1g62580), *FMO* (At1g12200) and *SDH1-1* (At5g66760) – was
801 produced with the open-source software R using the CRAN library package *qgraph*
802 (**Epskamp et al., 2012**). Correlation significance was tested with Minitab 17.

803

804 **GO Network Analyses**

805 AraNet (<http://www.inetbio.org/aranet>) is a free database of co-functional gene networks
806 based on *Arabidopsis thaliana* TAIR10 annotations (**Lee et al., 2015**), which can be
807 used for computational identification of new candidate genes in functional pathways and
808 for the integration of high-throughput omics datasets (**Lee et al., 2010**). Closely
809 connected genes are listed and ranked in a guilt-by-association network on the basis of
810 previous experimental datasets and Gene Ontology evidence codes, such as IDA
811 (inferred from direct assay), IPI (inferred from protein interaction), ISS (inferred from
812 sequence or structural similarity) and TAS (traceable author statement). Model accuracy

813 and coverage are assessed with the “receiver operating characteristic” (ROC) which
814 calculates the probability rate of true-positives versus false-positives, between the inter-
815 connectivity of the entry genes and a selection of random genes. The receiver operating
816 characteristic (ROC) calculates the model fitness for the connected genes, as true-
817 positives and false-positives rate between the entry genes (red curve) and a randomly
818 generated gene-set (green curve). The corresponding score of the “area under the ROC
819 curve” (AUC) ranges from ~0.5 to 1, respectively indicating random and perfect
820 performance. New candidate genes were searched with the function “*new members of a*
821 *pathway*”. The predictive power of the new network is automatically estimated from the
822 initial inter-connectivity of its genes, on the basis of the connection to the entry genes
823 (ranked by connectivity scores). The AraNet function “GeneSet analysis / GO” was used
824 to evaluate enrichment of the network. The same GO analysis function was also used to
825 confirm the network enrichment in glycerol and glycerolipid metabolic processes of the
826 gene-set selection (by enzyme substrate annotation; 76 genes) later used for
827 multivariate effects of the treatments. Results from the AraNet analysis were imported
828 into Cytoscape and colored according to statistically overrepresented GO categories
829 using the plugin GOlorize by (**Garcia et al., 2007**)

830 (<http://apps.cytoscape.org/apps/golorize>).

831 Another public web server was used for prediction of biological interaction namely
832 GeneMANIA (<http://www.genemania.org/>), which can also be used as a Cytoscape
833 plugin (**Warde-Farley et al., 2010**). The initial entry list consisted of the five genes
834 *GPDHc1* (At2g41540), *SDP6* (At3g10370), *NOGC1* (At1g62580), *FMO* (At1g12200)
835 constituting the core region of the glycerol network in analysis, and the predicted
836 interaction with *SDH1-1* (At5g66760). GeneMANIA extended this list to create a network

837 of genes identified as having similar functions. The predicted gene interactions and their
838 weights were estimated on the basis of *Arabidopsis* knowledge through genomics and
839 proteomics data (e.g. co-expression and protein interaction) which are retrieved from
840 GEO, BioGRID, Pathway Commons and I2D, as well as organism-specific functional
841 genomics data sets (Warde-Farley et al., 2010).

842

843 **Figure Layout and Editing**

844 Photoshop CS5.1© (Adobe) was used for editing the final graphic layouts of the figures.

845

846 **Accession Numbers**

847 Microarray data from the transcriptomics analysis were deposited in the ArrayExpress
848 database (www.ebi.ac.uk/arrayexpress) under accession number E-MTAB-5030.

849 Sequence data from this article can be found in the Arabidopsis Genome Initiative or

850 GenBank/EMBL databases under the following accession numbers: At2g30570 (*PSBW*),

851 At3g54890 (*LHCA1*), At1g19150 (*LHCA6*), At2g34420 (*LHB1B2*), At2g40100 (*LHCB4.3*),

852 At4g10340 (*LHCB5*), At1g15820 (*LHCB6*), At1g60950 (*FED A*), At1g08550 (*NPQ1*),

853 At1g07110 (*F2KP*), At2g21330 (*FBA1*), At4g38970 (*FBA2*), At3g54050 (*CFBP1/HCEF1*),

854 At2g25540 (*CESA10*), At4g16590 (*CSLA01*), At2g22900 (*MUC110*), At3g46970 (*PHS2*),

855 At5g37600 (*ATGSR1*), At2g29110 (*GLR2.8*), At2g29100 (*GLR2.9*), At3g01120 (*MTO1*),

856 At5g09220 (*AAP2*), At4g39660 (*AGT2*), At1g17290 (*ALAAT1*), At1g05940 (*CAT9*),

857 At1g20020 (*LFNR2*), At5g11670 (*ATNADP-ME2*), At5g09660 (*PMDH2*), At3g14420

858 (*GOX1*), At3g21070 (*NADK1*), At5g66760 (*SDH1-1*), At3g10920 (*MSD1*), At4g31800

859 (*WRKY18*), At1g80840 (*WRKY40*), At2g46400 (*WRKY46*), At3g45140 (*LOX2*),

860 At1g17420 (*LOX3*), At1g32640 (*MYC2*), At5g67300 (*MYB44*), At2g37630 (*MYB91*),

861 At1g72290 (*WSCP*), At3g45640 (*MPK3*), At5g45340 (*CYP707A3*), At5g47220 (*ERF2*),
862 At3g20770 (*EIN3*), AT2G02990 (*RNS1*), At2g38940 (*PT2*), At2g38170 (*CAX1*),
863 At1g68100 (*IAR1*), At1g62580 (*NOGC1*), At1g12200 (*FMO*), At1g29740 (*LRR-RK*),
864 At1g29310 (SecY protein/sec61), At2g15230 (*LIP1*), At2g41540 (*GPDHc1*), At3g10370
865 (*SDP6*), At3g18830 (*PLT5*), At5g13640 (*PDAT*), At3g11670 (*DGD1*), At5g01220 (*SQD2*),
866 At3g52430 (*PAD4*), At1g54100 (*ALDH7B4*), At2g37790 (*AKR4C10*), At2g10940 (*LTPc1*;
867 lipid-transfer protein; chloroplast), At2g45180 (*LTPc2*; lipid-transfer protein; chloroplast).

868

869 **Acknowledgments**

870 We thank the University of Lausanne and the University of Eastern Finland, and
871 particularly Timo Oksanen for technical support; the University of Umeå (UmU) and the
872 Umeå Plant Science Centre (UPSC) for the working environment. We thank the staff of
873 the Swedish Metabolomics Centre (SMC), particularly Krister Lundgren and Ilka Abreu
874 for technical assistance on the mass-spectrometry analyses, and Rui Climaco Pinto
875 (BILS) for assistance in the bioinformatic analysis and data evaluation. This work was
876 supported by the European Science Foundation which funded EUROCORES program
877 A-BIO-VOC (EuroVOL), and by national funds from the Vetenskapsrådet (VR/ESF 324-
878 2011-787 to B.A and T.M), the Academy of Finland (decision numbers 141053, 251898
879 to J.B.), and the Swiss National Science Foundation (decision numbers 31VL30_134414
880 to P.R.).

881 Papazian et al., 2016

882

883 Tables:

884 **Table I** Major hubs in the integrative network correlation analysis

885 **Table II** Biological processes relative to glycerol metabolic responses
886 **Table III** Photosynthetic and gas exchange measurements
887

Table I Major gene hubs in *Brassica nigra* network for multiple stress response to O₃ and herbivory (Fig. 4)

AGI		Gene name	GO Process ^a	Cellular location ^b
At4g27740	-	Yippee family putative zinc-binding	Unknown	Nucleus
At4g16590	<i>CSLA1</i>	Cellulose synthase-like A01	Glycosyl transferase	Golgi, Cytosol
At5g04440	-	Unknown function (DUF1997)	Unknown	Chloroplast
At1g12390	-	Cornichon protein (Guard cells)	Signal transduction	Plasma membrane
At2g29100	<i>GLR2.9</i>	Glutamate receptor 2.9	Ca ⁺⁺ homeostasis	Plasma membrane, Golgi, ER
At3g50830	<i>COR413</i>	Cold acclimation WCOR413-like	Unknown	Plasma membrane
At1g29910	<i>LHCB1.2</i>	Light harvest chlorophyll binding 1.2	Photosynthesis	Chloroplast
At2g22900	<i>MUCI10</i>	Mucilage-related 10	Galactosyltransferase	Golgi, trans-Golgi
At2g32990	<i>GH9B8</i>	Glycosyl hydrolase 9B8	Cellulose biosynthesis	Extracellular (Cell wall)
At3g09360	-	TBP-binding protein	RNA polymerase II (TF)	Nucleus
At1g62580	<i>NOGC1</i>	NO-dependent guanylate cyclase 1	Stomatal closure	Chloroplast, cytosol
At3g50770	<i>CML41</i>	Calmodulin-like 41	Signaling, Ca ⁺⁺ binding	Chloroplast
At5g58270	<i>M3</i>	ABC transporter mitochondrion 3	Mo-cofactor biosynthesis	Mitochondria, chloroplast
At3g24100	-	SERF (uncharacterized)	Unknown	Nucleus
At1g07040	-	Unknown protein	Unknown	Chloroplast
At2g02390	<i>GST18</i>	Glutathione S-transferase 18	Amino acid biosynthesis	Cytoplasm, cytosol

^aGO biological processes and/or molecular functions as reported by the TAIR database (<https://www.arabidopsis.org>).

^bCellular localization confirmed with ePlant visualization tool (BAR – University Toronto, <http://bar.utoronto.ca/~dev/eplant>).

888

889

Table II Biological processes relative to *Brassica nigra* glycerol metabolic network responsive to O₃ and herbivory

Rank	GO ID	Biological Process	P-value ^a	Genes
1	GO:0006636	Unsaturated fatty acid biosynthesis	0.0001632	<i>SQD2, LIP1, PDAT</i>
2	GO:0006127	Glycerol phosphate shuttle	0.0002918	<i>GPDHc1, SDP6</i>
3	GO:0016117	Carotenoid biosynthesis	0.0003421	<i>SQD2, LIP1, PDAT</i>
4	GO:0019375	Galactolipid biosynthesis	0.0003564	<i>DGD1, SQD2</i>
5	GO:0015995	Chlorophyll biosynthesis	0.0004397	<i>DGD1, SQD2, LIP1</i>
6	GO:0046506	Sulfolipid biosynthesis	0.0005835	<i>DGD1, SQD2</i>
7	GO:0016036	Phosphate starvation	0.0006321	<i>DGD1, SQD2</i>
8	GO:0019563	Glycerol catabolism	0.0008752	<i>GPDHc1, SDP6, LIP1</i>
9	GO:0042550	Photosystem I stabilization	0.0008752	<i>DGD1</i>
10	GO:0019761	Glucosinolate biosynthesis	0.0009609	<i>SQD2</i>
11	GO:0006072	Glycerol-3-phosphate metabolism	0.001167	<i>GPDHc1, SDP6</i>
12	GO:0009247	Glycolipid biosynthesis	0.001458	<i>DGD1, SQD2</i>
13	GO:0019288	Isopentenyl diphosphate biosynthesis (MEP pathway)	0.001849	<i>DGD1, SQD2</i>
14	GO:0090332	Stomatal closure	0.002915	<i>NOGC1</i>
15	GO:0006071	Glycerol metabolism	0.00466	<i>GPDHc1, SDP6</i>

^aGO terms P-value < 0.01 calculated in AraNet as hypergeometric test on all 27416 gene entries in the Arabidopsis database.

890

891

892

Table III Photosynthetic and gas exchange measurements of 5 weeks old *Brassica nigra*, under stress of O₃ and herbivory.

Treatment effect:	O ₃ (5 days, 70 ppb)		<i>P. brassicae</i> herbivory (24 hours)		O ₃ (16 days, 70 ppb)
	C	O (vs. C)	P (vs. C)	OP (vs. O)	OL (vs. C)
Photosynthesis ($\mu\text{mol CO}_2\text{m}^{-2}\text{s}^{-1}$)	11.72 ± 0.8	8.63 ± 0.63 **	11.5 ± 0.58 n.s.	11.24 ± 0.85 *	3.29 ± 0.26 ***
Stomatal conductance ($\text{mol H}_2\text{O m}^{-2}\text{s}^{-1}$)	0.31 ± 0.02	0.15 ± 0.04 **	0.25 ± 0.10 n.s.	0.24 ± 0.03 *	0.12 ± 0.01 **
Leaf transpiration ($\text{mol H}_2\text{O m}^{-2}\text{s}^{-1}$)	3.45 ± 0.22	1.84 ± 0.22 ***	2.97 ± 0.90 n.s.	2.66 ± 0.26 *	1.55 ± 0.19 ***
Intracellular CO ₂ concentration (ppm)	300 ± 3.87	264 ± 4.93 *	291 ± 9.35 n.s.	288 ± 9.81 n.s.	333 ± 10.19 ***

Means ± SE (n = 6-10) and significant variation calculated via student t-test, *P*-values > 0.05 (*), > 0.01 (**), > 0.001 (***).
Relative group comparisons as in brackets. Treatments abbreviations: controls (C), exposure to O₃ 70 ppb / 5 days (O),
exposure to O₃ 70 ppb / 16 days (OL), *P. brassicae* herbivory for 24 hours (P), sequential O₃ 70 ppb and herbivory (OP).

893

894

895 **Footnotes**

896 The authors responsible for distribution of materials integral to the findings presented in
897 this article in accordance with the policy described in the Instructions for Authors
898 (www.plantcell.org) are: Stefano Papazian (stefano.papazian@umu.se) and Benedicte
899 Albrechtsen (benedicte.albrechtsen@umu.se).

900
901 J.B. conceived the project; E.K., P.R, C.B., S.P. and B.A assisted in design the research;
902 J.B., S.P. and E.K. performed the experiments; S.P. C.B. and E.K. performed the
903 analyses; S.L. provided technical assistance to C.B; J.B., P.R., and T.M. supervised the
904 analyses; S.P. analyzed the data. B.A., C.B., and P.R. contributed statistical analyses.
905 S.P., J.B. and B.A. wrote the article with contributions of all the authors; P.R. and T.M
906 supervised and complemented the writing.

907

908

Parsed Citations

Abe, H., Urao, T., Ito, T., Seki, M., Shinozaki, K., and Yamaguchi-Shinozaki, K. (2003). Arabidopsis AtMYC2 (bHLH) and AtMYB2 (MYB) function as transcriptional activators in abscisic acid signaling. The Plant Cell 15, 63-78.

Pubmed: [Author and Title](#)

CrossRef: [Author and Title](#)

Google Scholar: [Author Only](#) [Title Only](#) [Author and Title](#)

Anderson, J.P. (2004). Antagonistic Interaction between Abscisic Acid and Jasmonate-Ethylene Signaling Pathways Modulates Defense Gene Expression and Disease Resistance in Arabidopsis. The Plant Cell Online 16, 3460-3479.

Pubmed: [Author and Title](#)

CrossRef: [Author and Title](#)

Google Scholar: [Author Only](#) [Title Only](#) [Author and Title](#)

Ansari, M., Lee, R.H., and Chen, S.C. (2005). A novel senescence-associated gene encoding γ -aminobutyric acid (GABA):pyruvate transaminase is upregulated during rice leaf senescence. Physiologia plantarum 123, 1-8.

Pubmed: [Author and Title](#)

CrossRef: [Author and Title](#)

Google Scholar: [Author Only](#) [Title Only](#) [Author and Title](#)

Ashmore M.R. (2005) Assessing the future global impacts of ozone on vegetation. Plant, Cell & Environment 28, 949-964.

Pubmed: [Author and Title](#)

CrossRef: [Author and Title](#)

Google Scholar: [Author Only](#) [Title Only](#) [Author and Title](#)

Assenov, Y., Ramírez, F., Schelhorn, S.E., Lengauer, T., Albrecht, M., (2008) Computing topological parameters of biological networks. Bioinformatics 24, 282-284,

Pubmed: [Author and Title](#)

CrossRef: [Author and Title](#)

Google Scholar: [Author Only](#) [Title Only](#) [Author and Title](#)

Atkinson, N.J., and Urwin, P.E. (2012). The interaction of plant biotic and abiotic stresses: from genes to the field. Journal of Experimental Botany 63, 3523-3543.

Pubmed: [Author and Title](#)

CrossRef: [Author and Title](#)

Google Scholar: [Author Only](#) [Title Only](#) [Author and Title](#)

Atkinson, N.J., Lilley, C.J., and Urwin, P.E. (2013). Identification of genes involved in the response of Arabidopsis to simultaneous biotic and abiotic stresses. Plant physiology 162, 2028-2041.

Pubmed: [Author and Title](#)

CrossRef: [Author and Title](#)

Google Scholar: [Author Only](#) [Title Only](#) [Author and Title](#)

Bagard, M., Thiec, D., Delacote, E., Hasenfratz-Sauder, M.P., Banvoy, J., Gérard, J., Dizengremel, P., and Jolivet, Y. (2008). Ozone-induced changes in photosynthesis and photorespiration of hybrid poplar in relation to the developmental stage of the leaves. Physiologia plantarum 134, 559-574.

Pubmed: [Author and Title](#)

CrossRef: [Author and Title](#)

Google Scholar: [Author Only](#) [Title Only](#) [Author and Title](#)

Baldoni, E., Genga, A., and Cominelli, E. (2015). Plant MYB Transcription Factors: Their Role in Drought Response Mechanisms. International journal of molecular sciences 16, 15811-15851.

Pubmed: [Author and Title](#)

CrossRef: [Author and Title](#)

Google Scholar: [Author Only](#) [Title Only](#) [Author and Title](#)

Bale, J.S., Masters, G.J., Hodkinson, I.D., Awmack, C., Bezemer, T.M., Brown, V.K., Butterfield, J., Buse, A., Coulson, J.C., Farrar, J., Good, J.E.G., Harrington, R., Hartley, S., Jones, T.H., Lindroth, R.L., Press, M.C., Symrnioudis, I., Watt, A.D., and Whittaker, J.B. (2002). Herbivory in global climate change research: direct effects of rising temperature on insect herbivores. Global Change Biol 8, 1-16.

Pubmed: [Author and Title](#)

CrossRef: [Author and Title](#)

Google Scholar: [Author Only](#) [Title Only](#) [Author and Title](#)

Barah, P., and Bones, A.M. (2014). Multidimensional approaches for studying plant defence against insects: from ecology to omics and synthetic biology. Journal of Experimental Botany 66, 479-493.

Pubmed: [Author and Title](#)

CrossRef: [Author and Title](#)

Google Scholar: [Author Only](#) [Title Only](#) [Author and Title](#)

Bekaert, M., Edger, P.P., Hudson, C.M., Pires, J.C., and Conant, G.C. (2012). Metabolic and evolutionary costs of herbivory defense: systems biology of glucosinolate synthesis. The New phytologist 196, 596-605.

Pubmed: [Author and Title](#)

CrossRef: [Author and Title](#)

Google Scholar: [Author Only](#) [Title Only](#) [Author and Title](#)

Bennett, R., Donald, A., Dawson, G., Hick, A., and Wallsgrove, R. (1993). Aldoxime-Forming Microsomal-Enzyme Systems Involved in the Biosynthesis of Glucosinolates in Oilseed Rape (Brassica-Napus) Leaves. Plant physiology 102, 1307-1312.

Pubmed: [Author and Title](#)

CrossRef: [Author and Title](#)
Google Scholar: [Author Only Title Only Author and Title](#)

Ben Rejeb, I., Pastor, V., Mauch-Mani, B. (2014). Plant responses to simultaneous biotic and abiotic stress: Molecular mechanisms. *Plants* 3, 458-475.

Pubmed: [Author and Title](#)
CrossRef: [Author and Title](#)
Google Scholar: [Author Only Title Only Author and Title](#)

Berg, J.M., Tymoczko, J.L., and Stryer, L. (2012). *Biochemistry*. (New York: W.H. Freeman). Chapter 18, Oxidative Phosphorylation.

Pubmed: [Author and Title](#)
CrossRef: [Author and Title](#)
Google Scholar: [Author Only Title Only Author and Title](#)

Bergmann, E., Bender, J., and Weigel, H.J. (1999). Ozone threshold doses and exposure-response relationships for the development of ozone injury symptoms in wild plant species. *New Phytologist* 144, 423-435.

Pubmed: [Author and Title](#)
CrossRef: [Author and Title](#)
Google Scholar: [Author Only Title Only Author and Title](#)

Biela, A., Grote, K., Otto, B., Hoth, S., Hedrich, R., and Kaldenhoff, R. (1999). The *Nicotiana tabacum* plasma membrane aquaporin NtAQP1 is mercury-insensitive and permeable for glycerol. *The Plant journal : for cell and molecular biology* 18, 565-570.

Pubmed: [Author and Title](#)
CrossRef: [Author and Title](#)
Google Scholar: [Author Only Title Only Author and Title](#)

Bilgin, D.D., Zavala, J.A., Zhu, J.I.N., Clough, S.J., Ort, D.R., and DeLucia, E.H. (2010). Biotic stress globally downregulates photosynthesis genes. *Plant, Cell and Environment* 33, 1597-1613.

Pubmed: [Author and Title](#)
CrossRef: [Author and Title](#)
Google Scholar: [Author Only Title Only Author and Title](#)

Bino, R.J., Hall, R.D., Fiehn, O., Kopka, J., Saito, K., Draper, J., Nikolau, B.J., Mendes, P., Roessner-Tunali, U., Beale, M.H., Trethewey, R.N., Lange, B.M., Wurtele, E.S., and Sumner, L.W. (2004). Potential of metabolomics as a functional genomics tool. *Trends in plant science* 9, 418-425.

Pubmed: [Author and Title](#)
CrossRef: [Author and Title](#)
Google Scholar: [Author Only Title Only Author and Title](#)

Bodenhorn N., Reymond P. (2007). Signaling Pathways Controlling Induced Resistance to Insect Herbivores in *Arabidopsis*, *Molecular Plant-Microbe Interactions* 20, 1406-1420.

Pubmed: [Author and Title](#)
CrossRef: [Author and Title](#)
Google Scholar: [Author Only Title Only Author and Title](#)

Boeckler, G.A., Gershenzon, J., and Unsicker, S.B. (2011). Phenolic glycosides of the Salicaceae and their role as anti-herbivore defenses. *Phytochemistry* 72, 1497-1509.

Pubmed: [Author and Title](#)
CrossRef: [Author and Title](#)
Google Scholar: [Author Only Title Only Author and Title](#)

Boex-Fontvieille, E., Rustgi, S., von Wettstein, D., Reinbothe, S., and Reinbothe, C. (2015). Water-soluble chlorophyll protein is involved in herbivore resistance activation during greening of *Arabidopsis thaliana*. *Proceedings of the National Academy of Sciences of the United States of America* 112, 7303-7308.

Pubmed: [Author and Title](#)
CrossRef: [Author and Title](#)
Google Scholar: [Author Only Title Only Author and Title](#)

Booker F, Muntifering R, McGrath M, Burkey K, Decoteau D, Fiscus E, Manning W, Krupa S, Chappelka A, Grantz D. (2009). The ozone component of global change: potential effects on agricultural and horticultural plant yield, product quality and interactions with invasive species. *Journal of Integrative Plant Biology* 51, 337-51.

Pubmed: [Author and Title](#)
CrossRef: [Author and Title](#)
Google Scholar: [Author Only Title Only Author and Title](#)

Both M., Csukai M., Stumpf M.P., Spanu P.D. (2005) Gene expression profiles of *Blumeria graminis* indicate dynamic changes to primary metabolism during development of an obligate biotrophic pathogen. *Plant Cell*. 17, 2107-2122.

Pubmed: [Author and Title](#)
CrossRef: [Author and Title](#)
Google Scholar: [Author Only Title Only Author and Title](#)

Bouché, N., Fait, A., and Bouchez, D. (2003). Mitochondrial succinic-semialdehyde dehydrogenase of the γ -aminobutyrate shunt is required to restrict levels of reactive oxygen intermediates in plants. *Proceedings of the National Academy of Sciences of the United States of America* 27, 6843-6848

Pubmed: [Author and Title](#)
CrossRef: [Author and Title](#)
Google Scholar: [Author Only Title Only Author and Title](#)

Bouché, N., and Fromm, H. (2004). GABA in plants: just a metabolite? *Trends in plant science* 9, 110-115.

Pubmed: [Author and Title](#)

CrossRef: [Author and Title](#)
Google Scholar: [Author Only Title Only Author and Title](#)

Breeze, E., Harrison, E., McHattie, S., Hughes, L., Hickman, R., Hill, C., Kiddle, S., Kim, Y.-s., Penfold, C.A., Jenkins, D., Zhang, C., Morris, K., Jenner, C., Jackson, S., Thomas, B., Tabrett, A., Legaie, R., Moore, J.D., Wild, D.L., Ott, S., Rand, D., Beynon, J., Denby, K., Mead, A., and Buchanan-Wollaston, V. (2011). High-Resolution Temporal Profiling of Transcripts during Arabidopsis Leaf Senescence Reveals a Distinct Chronology of Processes and Regulation. *The Plant Cell Online* 23, 873-894.

Pubmed: [Author and Title](#)
CrossRef: [Author and Title](#)
Google Scholar: [Author Only Title Only Author and Title](#)

Castagna, A., and Ranieri, A. (2009). Detoxification and repair process of ozone injury: from O₃ uptake to gene expression adjustment. *Environmental pollution (Barking, Essex : 1987)* 157, 1461-1469.

Pubmed: [Author and Title](#)
CrossRef: [Author and Title](#)
Google Scholar: [Author Only Title Only Author and Title](#)

Chen, H., Chen, S.-L., and Jiang, J.-G. (2011). Effect of Ca²⁺ Channel Block on Glycerol Metabolism in *Dunaliella salina* under Hypoosmotic and Hyperosmotic Stresses. *Plos One* 6.

Pubmed: [Author and Title](#)
CrossRef: [Author and Title](#)
Google Scholar: [Author Only Title Only Author and Title](#)

Clarke, D.B. (2010). Glucosinolates, structures and analysis in food. *Analytical Methods* 2, 310-325.

Pubmed: [Author and Title](#)
CrossRef: [Author and Title](#)
Google Scholar: [Author Only Title Only Author and Title](#)

Consales, F., Schweizer, F., Erb, M., Gouhier-Darimont, C., Bodenhausen, N., Bruessow, F., Sobhy, I., and Reymond, P. (2012). Insect oral secretions suppress wound-induced responses in Arabidopsis. *Journal of Experimental Botany* 63, 727-737.

Pubmed: [Author and Title](#)
CrossRef: [Author and Title](#)
Google Scholar: [Author Only Title Only Author and Title](#)

Debouba, M., Dguimi, H.M., Ghorbel, M., Gouia, H., and Suzuki, A. (2013). Expression pattern of genes encoding nitrate and ammonium assimilating enzymes in Arabidopsis thaliana exposed to short term NaCl stress. *Journal of plant physiology* 170, 155-160.

Pubmed: [Author and Title](#)
CrossRef: [Author and Title](#)
Google Scholar: [Author Only Title Only Author and Title](#)

de Vos, M., van Oosten, V.R., van Poecke, R.M.P., van Pelt, J.A., Pozo, M.J., Mueller, M.J., Buchara, A.J., Métraux, J-P., van Loon, L.C., Dicke, M., and Pieterse, C.M.J. (2005) Signal Signature and Transcriptome Changes of Arabidopsis During Pathogen and Insect Attack. *Molecular and Plant-Microbe Interactions* 18: 923-927.

Pubmed: [Author and Title](#)
CrossRef: [Author and Title](#)
Google Scholar: [Author Only Title Only Author and Title](#)

Ditchkoff, S.S., Lewis, J.S., Lin, J.C., Muntifering, R.B., and Chappelka, A.H. (2009). Nutritive Quality of Highbush Blackberry (*Rubus argutus*) Exposed to Tropospheric Ozone. *Rangeland Ecol Manag* 62, 364-370.

Pubmed: [Author and Title](#)
CrossRef: [Author and Title](#)
Google Scholar: [Author Only Title Only Author and Title](#)

Dizengremel, P., Le Thiec, D., Bagard, M., and Jolivet, Y. (2008). Ozone risk assessment for plants: Central role of metabolism-dependent changes in reducing power. *Environmental Pollution* 156, 11-15.

Pubmed: [Author and Title](#)
CrossRef: [Author and Title](#)
Google Scholar: [Author Only Title Only Author and Title](#)

Dizengremel P., Le Thiec D., Hasenfratz-Sauder M.P., Vaultier M.N., Bagard M., Jolivet Y. (2009). Metabolic-dependent changes in plant cell redox power after ozone exposure. *Plant Biology* 11, 35-42.

Pubmed: [Author and Title](#)
CrossRef: [Author and Title](#)
Google Scholar: [Author Only Title Only Author and Title](#)

Dizengremel, P., Vaultier, M.-N.N., Le Thiec, D., Cabané, M., Bagard, M., Gérard, D., Gérard, J., Dghim, A.A., Richet, N., Afif, D., Pireaux, J.-C.C., Hasenfratz-Sauder, M.-P.P., and Jolivet, Y. (2012). Phosphoenolpyruvate is at the crossroads of leaf metabolic responses to ozone stress. *The New phytologist* 195, 512-517.

Pubmed: [Author and Title](#)
CrossRef: [Author and Title](#)
Google Scholar: [Author Only Title Only Author and Title](#)

Dombrecht, B., Xue, G.P., Sprague, S.J., Kirkegaard, J.A., Ross, J.J., Reid, J.B., Fitt, G.P., Sewelam, N., Schenk, P.M., Manners, J.M., and Kazan, K. (2007). MYC2 differentially modulates diverse jasmonate-dependent functions in Arabidopsis. *The Plant Cell* 19, 2225-2245.

Pubmed: [Author and Title](#)
CrossRef: [Author and Title](#)
Google Scholar: [Author Only Title Only Author and Title](#)

Draborg, H., Villadsen, D., and Nielsen, T.H. (2001). Transgenic *Arabidopsis* plants with decreased activity of fructose-6-phosphate,2-kinase/fructose-2,6-bisphosphatase have altered carbon partitioning. *Plant physiology* 126, 750-758.

Pubmed: [Author and Title](#)

CrossRef: [Author and Title](#)

Google Scholar: [Author Only](#) [Title Only](#) [Author and Title](#)

Eastmond, P.J. (2004). Glycerol insensitive *Arabidopsis* mutants: gli1 seedlings lack glycerol kinase, accumulate glycerol and are more resistant to abiotic stress. *The Plant Journal* 37, 617-625.

Pubmed: [Author and Title](#)

CrossRef: [Author and Title](#)

Google Scholar: [Author Only](#) [Title Only](#) [Author and Title](#)

El-Kouhen, K., Blangy, S., Ortiz, E., Gardies, A.-M., Ferté, N., and Arondel, V. (2005). Identification and characterization of a triacylglycerol lipase in *Arabidopsis* homologous to mammalian acid lipases. *FEBS letters* 579, 6067-6073.

Pubmed: [Author and Title](#)

CrossRef: [Author and Title](#)

Google Scholar: [Author Only](#) [Title Only](#) [Author and Title](#)

Epskamp, S., Cramer, A.O.J., Waldorp, L.J., Schmittmann, V.D., and Borsboom, D. (2012). qgraph: Network Visualizations of Relationships in Psychometric Data. *J Stat Softw* 48, 1-18.

Pubmed: [Author and Title](#)

CrossRef: [Author and Title](#)

Google Scholar: [Author Only](#) [Title Only](#) [Author and Title](#)

Fahey, J.W., Zalcmann, A.T., and Talalay, P. (2001). The chemical diversity and distribution of glucosinolates and isothiocyanates among plants. *Phytochemistry* 56, 5-51.

Pubmed: [Author and Title](#)

CrossRef: [Author and Title](#)

Google Scholar: [Author Only](#) [Title Only](#) [Author and Title](#)

Fait, A., Fromm, H., Walter, D., Galili, G., and Fernie, A.R. (2008). Highway or byway: the metabolic role of the GABA shunt in plants. *Trends in plant science* 13, 14-19.

Pubmed: [Author and Title](#)

CrossRef: [Author and Title](#)

Google Scholar: [Author Only](#) [Title Only](#) [Author and Title](#)

Fares, S., Oksanen, E., Lannenpaa, M., Julkunen-Tiitto, R., and Loreto, F. (2010). Volatile emissions and phenolic compound concentrations along a vertical profile of *Populus nigra* leaves exposed to realistic ozone concentrations. *Photosynthesis research* 104, 61-74.

Pubmed: [Author and Title](#)

CrossRef: [Author and Title](#)

Google Scholar: [Author Only](#) [Title Only](#) [Author and Title](#)

Felton, G.W., Bi, J.L., Summers, C.B., Mueller, A.J., and Duffey, S.S. (1993). Potential role of lipoxygenases in defense against insect herbivory. *Journal of chemical ecology* 20, 651-666.

Pubmed: [Author and Title](#)

CrossRef: [Author and Title](#)

Google Scholar: [Author Only](#) [Title Only](#) [Author and Title](#)

Fernandez O., Béthencourt L., Quero A, Sangwan R.S., Clément C. (2010). Trehalose and plant stress responses: friend or foe? *Trends in Plant Science* 15, 409-417.

Pubmed: [Author and Title](#)

CrossRef: [Author and Title](#)

Google Scholar: [Author Only](#) [Title Only](#) [Author and Title](#)

Fiehn, O. (2002). Metabolomics - the link between genotypes and phenotypes. *Plant molecular biology* 48, 155-171.

Pubmed: [Author and Title](#)

CrossRef: [Author and Title](#)

Google Scholar: [Author Only](#) [Title Only](#) [Author and Title](#)

Firn, R.D., and Jones, C.G. (2009). A Darwinian view of metabolism: molecular properties determine fitness. *J Exp Bot* 60, 719-726.

Pubmed: [Author and Title](#)

CrossRef: [Author and Title](#)

Google Scholar: [Author Only](#) [Title Only](#) [Author and Title](#)

Forde, B.G., and Lea, P.J. (2007). Glutamate in plants: metabolism, regulation, and signalling. *Journal of Experimental Botany* 58, 2339-2358.

Pubmed: [Author and Title](#)

CrossRef: [Author and Title](#)

Google Scholar: [Author Only](#) [Title Only](#) [Author and Title](#)

Fuhrer, J. (2003). Agroecosystem responses to combinations of elevated CO₂, ozone, and global climate change. *Agriculture, Ecosystems & Environment* 97, 1-20.

Pubmed: [Author and Title](#)

CrossRef: [Author and Title](#)

Google Scholar: [Author Only](#) [Title Only](#) [Author and Title](#)

Fujimoto, S.Y., Ohta, M., Usui, A., Shinshi, H., and Ohme-Takagi, M. (2000). *Arabidopsis* ethylene-responsive element binding factors act as transcriptional activators or repressors of GCC box-mediated gene expression. *The Plant cell* 12, 393-404.

Pubmed: [Author and Title](#)

CrossRef: [Author and Title](#)
Google Scholar: [Author Only Title Only Author and Title](#)

Fujita, M., Fujita, Y., Noutoshi, Y., Takahashi, F., Narusaka, Y., Yamaguchi-Shinozaki, K., and Shinozaki, K. (2006). Crosstalk between abiotic and biotic stress responses: a current view from the points of convergence in the stress signaling networks. *Current opinion in plant biology* 9, 436-442.

Pubmed: [Author and Title](#)
CrossRef: [Author and Title](#)
Google Scholar: [Author Only Title Only Author and Title](#)

Fukushima, A., Kusano, M., Redestig, H., Arita, M., and Saito, K. (2009). Integrated omics approaches in plant systems biology. *Current opinion in chemical biology* 13, 532-538.

Pubmed: [Author and Title](#)
CrossRef: [Author and Title](#)
Google Scholar: [Author Only Title Only Author and Title](#)

Garcia, O., Saveanu, C., Cline, M., Fromont-Racine, M., Jacquier, A., Schwikowski, B., and Aittokallio, T. (2007). Golorize: a Cytoscape plug-in for network visualization with Gene Ontology-based layout and coloring. *Bioinformatics* 23, 394-396.

Pubmed: [Author and Title](#)
CrossRef: [Author and Title](#)
Google Scholar: [Author Only Title Only Author and Title](#)

Geijer, C., Ahmadpour, D., Palmgren, M., Filipsson, C., Klein, D.M., Tamás, M.J., Hohmann, S., and Lindkvist-Petersson, K. (2012). Yeast aquaglyceroporins use the transmembrane core to restrict glycerol transport. *The Journal of biological chemistry* 287, 23562-23570.

Pubmed: [Author and Title](#)
CrossRef: [Author and Title](#)
Google Scholar: [Author Only Title Only Author and Title](#)

Geilen, K., and Bohmer, M. (2015). Dynamic subnuclear relocalization of WRKY40, a potential new mechanism of ABA-dependent transcription factor regulation. *Plant signaling & behavior* 10, e1106659.

Pubmed: [Author and Title](#)
CrossRef: [Author and Title](#)
Google Scholar: [Author Only Title Only Author and Title](#)

Gomes de Oliveira Dal'Molin, C., Quek, L.-E.E., Saa, P.A., and Nielsen, L.K. (2015). A multi-tissue genome-scale metabolic modeling framework for the analysis of whole plant systems. *Frontiers in plant science* 6, 4.

Pubmed: [Author and Title](#)
CrossRef: [Author and Title](#)
Google Scholar: [Author Only Title Only Author and Title](#)

Goumenaki, E., Taybi, T., Borland, A., and Barnes, J. (2010). Mechanisms underlying the impacts of ozone on photosynthetic performance. *Environmental and Experimental Botany* 69, 259-266.

Pubmed: [Author and Title](#)
CrossRef: [Author and Title](#)
Google Scholar: [Author Only Title Only Author and Title](#)

Halitschke, R., and Baldwin, I.T. (2003). Antisense LOX expression increases herbivore performance by decreasing defense responses and inhibiting growth-related transcriptional reorganization in *Nicotiana attenuata*. *The Plant Journal* 36, 794-807.

Pubmed: [Author and Title](#)
CrossRef: [Author and Title](#)
Google Scholar: [Author Only Title Only Author and Title](#)

Halitschke, R., Hamilton, J.G., and Kessler, A. (2011). Herbivore-specific elicitation of photosynthesis by mirid bug salivary secretions in the wild tobacco *Nicotiana attenuata*. *The New phytologist* 191, 528-535.

Pubmed: [Author and Title](#)
CrossRef: [Author and Title](#)
Google Scholar: [Author Only Title Only Author and Title](#)

Halkier, B., and Gershenzon, J. (2006). Biology and biochemistry of glucosinolates. *Annual review of plant biology* 57, 303-333.

Pubmed: [Author and Title](#)
CrossRef: [Author and Title](#)
Google Scholar: [Author Only Title Only Author and Title](#)

Havko, N.E., Major, I.T., Jewell, J.B., Attaran, E., Browse, J., and Howe, G.A. (2016). Control of Carbon Assimilation and Partitioning by Jasmonate: An Accounting of Growth-Defense Tradeoffs. *Plants* 5, 7.

Pubmed: [Author and Title](#)
CrossRef: [Author and Title](#)
Google Scholar: [Author Only Title Only Author and Title](#)

Hernández, I., and Munné-Bosch, S. (2015). Linking phosphorus availability with photo-oxidative stress in plants. *Journal of Experimental Botany* 66, 2889-2900.

Pubmed: [Author and Title](#)
CrossRef: [Author and Title](#)
Google Scholar: [Author Only Title Only Author and Title](#)

Hirai, M.Y., Sugiyama, K., Sawada, Y., Tohge, T., Obayashi, T., Suzuki, A., Araki, R., Sakurai, N., Suzuki, H., Aoki, K., Goda, H., Nishizawa, O.I., Shibata, D., and Saito, K. (2007). Omics-based identification of *Arabidopsis* Myb transcription factors regulating aliphatic glucosinolate biosynthesis. *Proceedings of the National Academy of Sciences of the United States of America* 104, 6478-6483.

Pubmed: [Author and Title](#)
CrossRef: [Author and Title](#)
Google Scholar: [Author Only](#) [Title Only](#) [Author and Title](#)

Hirner, B., Fischer, W.N., Rentsch, D., Kwart, M., and Frommer, W.B. (1998). Developmental control of H⁺/amino acid permease gene expression during seed development of Arabidopsis. The Plant Journal 14, 535-544.

Pubmed: [Author and Title](#)
CrossRef: [Author and Title](#)
Google Scholar: [Author Only](#) [Title Only](#) [Author and Title](#)

Hoefnagel, M., Atkin, O.K., and Wiskich, J.T. (1998). Interdependence between chloroplasts and mitochondria in the light and the dark. Biochimica et Biophysica Acta (BBA) - Bioenergetics 1366, 235-255.

Pubmed: [Author and Title](#)
CrossRef: [Author and Title](#)
Google Scholar: [Author Only](#) [Title Only](#) [Author and Title](#)

Hu, J., Zhang, Y., Wang, J., and Zhou, Y. (2014). Glycerol Affects Root Development through Regulation of Multiple Pathways in Arabidopsis. Plos One 9.

Pubmed: [Author and Title](#)
CrossRef: [Author and Title](#)
Google Scholar: [Author Only](#) [Title Only](#) [Author and Title](#)

Huang, S., Taylor, N.L., Stroher, E., Fenske, R., and Millar, A.H. (2013). Succinate dehydrogenase assembly factor 2 is needed for assembly and activity of mitochondrial complex II and for normal root elongation in Arabidopsis. The Plant journal : for cell and molecular biology 73, 429-441.

Pubmed: [Author and Title](#)
CrossRef: [Author and Title](#)
Google Scholar: [Author Only](#) [Title Only](#) [Author and Title](#)

Hui, D.Q., Iqbal J., Lehmann K., Gase K., Saluz H.P., Baldwin I.T. (2003). Molecular interactions between the specialist herbivore *Manduca sexta* (Lepidoptera, Sphingidae) and its natural host *Nicotiana attenuata*. V. Microarray analysis and further characterization of large-scale changes in herbivore-induced mRNAs. Plant Physiology 131, 1877-1893.

Pubmed: [Author and Title](#)
CrossRef: [Author and Title](#)
Google Scholar: [Author Only](#) [Title Only](#) [Author and Title](#)

Hummel, J., Strehmel, N., Selbig, J., Walther, D., and Kopka, J. (2010). Decision tree supported substructure prediction of metabolites from GC-MS profiles. Metabolomics 6, 322-333.

Pubmed: [Author and Title](#)
CrossRef: [Author and Title](#)
Google Scholar: [Author Only](#) [Title Only](#) [Author and Title](#)

Irmisch, S., McCormick, A.C., Gunther, J., Schmidt, A., Boeckler, G.A., Gershenzon, J., Unsicker, S.B., and Kollner, T.G. (2014). Herbivore-induced poplar cytochrome P450 enzymes of the CYP71 family convert aldoximes to nitriles which repel a generalist caterpillar. Plant Journal 80, 1095-1107.

Pubmed: [Author and Title](#)
CrossRef: [Author and Title](#)
Google Scholar: [Author Only](#) [Title Only](#) [Author and Title](#)

Jansen, J.J., Allwood, J.W., Marsden-Edwards, E., van der Putten, W.H., Goodacre, R., and van Dam, N.M. (2008). Metabolomic analysis of the interaction between plants and herbivores. Metabolomics 5, 150-161.

Pubmed: [Author and Title](#)
CrossRef: [Author and Title](#)
Google Scholar: [Author Only](#) [Title Only](#) [Author and Title](#)

Jaradat, M.R., Feurtado, J.A., Huang, D., Lu, Y., and Cutler, A.J. (2013). Multiple roles of the transcription factor *AtMYBR1/AtMYB44* in ABA signaling, stress responses, and leaf senescence. BMC Plant Biology 13, 192.

Pubmed: [Author and Title](#)
CrossRef: [Author and Title](#)
Google Scholar: [Author Only](#) [Title Only](#) [Author and Title](#)

Jost, R., Pharmawati, M., Lapis-Gaza, H.R., Rossig, C., Berkowitz, O., Lambers, H., and Finnegan, P.M. (2015). Differentiating phosphate-dependent and phosphate-independent systemic phosphate-starvation response networks in *Arabidopsis thaliana* through the application of phosphite. Journal of Experimental Botany 66, 2501-2514.

Pubmed: [Author and Title](#)
CrossRef: [Author and Title](#)
Google Scholar: [Author Only](#) [Title Only](#) [Author and Title](#)

Joudoi, T., Shichiri, Y., Kamizono, N., Akaike, T., Sawa, T., Yoshitake, J., Yamada, N., and Iwai, S. (2013). Nitrated Cyclic GMP Modulates Guard Cell Signaling in Arabidopsis. The Plant Cell 25, 558-571.

Pubmed: [Author and Title](#)
CrossRef: [Author and Title](#)
Google Scholar: [Author Only](#) [Title Only](#) [Author and Title](#)

Jouhet, J., Marechal, E., Baldan, B., Bligny, R., Joyard, J., and Block, M.A. (2004). Phosphate deprivation induces transfer of DGDG galactolipid from chloroplast to mitochondria. The Journal of cell biology 167, 863-874.

Pubmed: [Author and Title](#)
CrossRef: [Author and Title](#)
Google Scholar: [Author Only](#) [Title Only](#) [Author and Title](#)

Jung, C., Seo, J.S., Han, S.W., Koo, Y.J., Kim, C.H., Song, S.I., Nahm, B.H., Choi, Y.D., and Cheong, J.J. (2008). Overexpression of *AtMYB44* enhances stomatal closure to confer abiotic stress tolerance in transgenic *Arabidopsis*. *Plant physiology* 146, 623-635.

Pubmed: [Author and Title](#)

CrossRef: [Author and Title](#)

Google Scholar: [Author Only](#) [Title Only](#) [Author and Title](#)

Jung, C., Shim, J.S., Seo, J.S., Lee, H.Y., Kim, C.H., Choi, Y.D., and Cheong, J.-J. (2010). Non-specific phytohormonal induction of *AtMYB44* and suppression of jasmonate-responsive gene activation in *Arabidopsis thaliana*. *Molecules and cells* 29, 71-76.

Pubmed: [Author and Title](#)

CrossRef: [Author and Title](#)

Google Scholar: [Author Only](#) [Title Only](#) [Author and Title](#)

Kachroo, A., Venugopal, S.C., Lapchyk, L., Falcone, D., Hildebrand, D., and Kachroo, P. (2004). Oleic acid levels regulated by glycerolipid metabolism modulate defense gene expression in *Arabidopsis*. *Proceedings of the National Academy of Sciences of the United States of America* 101, 5152-5157.

Pubmed: [Author and Title](#)

CrossRef: [Author and Title](#)

Google Scholar: [Author Only](#) [Title Only](#) [Author and Title](#)

Kanehisa, M., and Goto, S. (2000). KEGG: kyoto encyclopedia of genes and genomes. *Nucleic acids research* 28, 27-30.

Pubmed: [Author and Title](#)

CrossRef: [Author and Title](#)

Google Scholar: [Author Only](#) [Title Only](#) [Author and Title](#)

Kangasjärvi, J., Jaspers, P., Kollist, H. (2005) Signalling and cell death in ozone-exposed plants. *Plant Cell and Environment* 28, 1021-1036.

Pubmed: [Author and Title](#)

CrossRef: [Author and Title](#)

Google Scholar: [Author Only](#) [Title Only](#) [Author and Title](#)

Karban, R., and Agrawal, A.A. (2002). Herbivore offense. *Annual Review of Ecology and Systematics* 33, 641-664.

Pubmed: [Author and Title](#)

CrossRef: [Author and Title](#)

Google Scholar: [Author Only](#) [Title Only](#) [Author and Title](#)

Khaling, E., Papazian, S., Poelman, E.H., Holopainen, J.K., Albrechtsen, B.R., and Blande, J.D. (2015). Ozone affects growth and development of *Pieris brassicae* on the wild host plant *Brassica nigra*. *Environ Pollut* 199, 119-129.

Pubmed: [Author and Title](#)

CrossRef: [Author and Title](#)

Google Scholar: [Author Only](#) [Title Only](#) [Author and Title](#)

Kim, J., Chang, C., and Tucker, M.L. (2015). To grow old: regulatory role of ethylene and jasmonic acid in senescence. *Frontiers in plant science* 6.

Pubmed: [Author and Title](#)

CrossRef: [Author and Title](#)

Google Scholar: [Author Only](#) [Title Only](#) [Author and Title](#)

Kleijn, R.J., Geertman, J.-M.A.M., Nfor, B.K., Ras, C., Schipper, D., Pronk, J.T., Heijnen, J.J., van Maris, A.J., and van Winden, W.A. (2007). Metabolic flux analysis of a glycerol-overproducing *Saccharomyces cerevisiae* strain based on GC-MS, LC-MS and NMR-derived C-labelling data. *FEMS yeast research* 7, 216-231.

Pubmed: [Author and Title](#)

CrossRef: [Author and Title](#)

Google Scholar: [Author Only](#) [Title Only](#) [Author and Title](#)

Koricheva, J. (2002). Meta-analysis of sources of variation in fitness costs of plant antiherbivore defenses. *Ecology* 83, 176-190.

Pubmed: [Author and Title](#)

CrossRef: [Author and Title](#)

Google Scholar: [Author Only](#) [Title Only](#) [Author and Title](#)

Kotchoni, S.O., Kuhns, C., Ditzer, A., Kirch, H.H., Bartels, D. (2006) Over-expression of different aldehyde dehydrogenase genes in *Arabidopsis thaliana* confers tolerance to abiotic stress and protects plants against lipid peroxidation and oxidative stress. *Plant Cell and Environment* 29, 1033-48.

Pubmed: [Author and Title](#)

CrossRef: [Author and Title](#)

Google Scholar: [Author Only](#) [Title Only](#) [Author and Title](#)

Lancien, M., and Roberts, M.R. (2006). Regulation of *Arabidopsis thaliana* 14-3-3 gene expression by gamma-aminobutyric acid. *Plant Cell and Environment* 29, 1430-1436.

Pubmed: [Author and Title](#)

CrossRef: [Author and Title](#)

Google Scholar: [Author Only](#) [Title Only](#) [Author and Title](#)

Lee, I., Ambaru, B., Thakkar, P., Marcotte, E.M., and Rhee, S.Y. (2010). Rational association of genes with traits using a genome-scale gene network for *Arabidopsis thaliana*. *Nat Biotechnol* 28, 149-U114.

Pubmed: [Author and Title](#)

CrossRef: [Author and Title](#)

Google Scholar: [Author Only](#) [Title Only](#) [Author and Title](#)

Lee, T., Yang, S., Kim, E., Ko, Y., Hwang, S., Shin, J., Shim, J.E., Shim, H., Kim, H., Kim, C., and Lee, I. (2015). AraNet v2: an improved database of co-functional gene networks for the study of *Arabidopsis thaliana* and 27 other nonmodel plant species.

Nucleic acids research 43, 996-1002.

Pubmed: [Author and Title](#)
CrossRef: [Author and Title](#)
Google Scholar: [Author Only](#) [Title Only](#) [Author and Title](#)

Li, D., Li, Y., Zhang, L., Wang, X., Zhao, Z., Tao, Z., Wang, J., Lin, M., Li, X., and Yang, Y. (2014). Arabidopsis ABA receptor RCAR1/PYL9 interacts with an R2R3-type MYB transcription factor, AtMYB44. *International journal of molecular sciences* 15, 8473-8490.

Pubmed: [Author and Title](#)
CrossRef: [Author and Title](#)
Google Scholar: [Author Only](#) [Title Only](#) [Author and Title](#)

Li, Q., Zheng, Q., Shen, W., Cram, D., Fowler, B.D., Wei, Y., and Zou, J. (2015). Understanding the Biochemical Basis of Temperature-Induced Lipid Pathway Adjustments in Plants. *The Plant Cell* 27, 86-103.

Pubmed: [Author and Title](#)
CrossRef: [Author and Title](#)
Google Scholar: [Author Only](#) [Title Only](#) [Author and Title](#)

Li, R.J., Hua, W., and Lu, Y.T. (2006). Arabidopsis cytosolic glutamine synthetase AtGLN1;1 is a potential substrate of AtCRK3 involved in leaf senescence. *Biochemical and biophysical research communications* 342, 119-126.

Pubmed: [Author and Title](#)
CrossRef: [Author and Title](#)
Google Scholar: [Author Only](#) [Title Only](#) [Author and Title](#)

Li, Z., Peng, J., Wen, X., and Guo, H. (2013). Ethylene-insensitive3 is a senescence-associated gene that accelerates age-dependent leaf senescence by directly repressing miR164 transcription in Arabidopsis. *The Plant Cell* 25, 3311-3328.

Pubmed: [Author and Title](#)
CrossRef: [Author and Title](#)
Google Scholar: [Author Only](#) [Title Only](#) [Author and Title](#)

Liechti, R., Csardi, G., Bergmann, S., Schutz, F., Sengstag, T., Boj, S. F., Servitja, J-M., Ferre, J., Van Lommel, L., Schuit, F., Klinger, S., Thorens, B., Naamane, N., Eizirik, D. L., Marselli, L., Bugliani, M., Marchetti, P., Lucas, S., Holm, C., Jongeneel, C. V., Xenarios, I. (2010). EuroDia: a beta-cell gene expression resource. *Database (Oxford)*.

Pubmed: [Author and Title](#)
CrossRef: [Author and Title](#)
Google Scholar: [Author Only](#) [Title Only](#) [Author and Title](#)

Lin, L.Z., Sun, J., Chen, P., and Harnly, J. (2011). UHPLC-PDA-ESI/HRMS/MS(n) analysis of anthocyanins, flavonol glycosides, and hydroxycinnamic acid derivatives in red mustard greens (*Brassica juncea* Coss variety). *Journal of agricultural and food chemistry* 59, 12059-12072.

Pubmed: [Author and Title](#)
CrossRef: [Author and Title](#)
Google Scholar: [Author Only](#) [Title Only](#) [Author and Title](#)

Lindroth, R.L. (2010). Impacts of Elevated Atmospheric CO₂ and O₃ on Forests: Phytochemistry, Trophic Interactions, and Ecosystem Dynamics. *Journal of chemical ecology* 36, 2-21.

Pubmed: [Author and Title](#)
CrossRef: [Author and Title](#)
Google Scholar: [Author Only](#) [Title Only](#) [Author and Title](#)

Liu, Z.Q., Yan, L., Wu, Z., Mei, C., Lu, K., Yu, Y.T., Liang, S., Zhang, X.F., Wang, X.F., and Zhang, D.P. (2012). Cooperation of three WRKY-domain transcription factors WRKY18, WRKY40, and WRKY60 in repressing two ABA-responsive genes ABI4 and ABI5 in Arabidopsis. *Journal of Experimental Botany* 63, 6371-6392.

Pubmed: [Author and Title](#)
CrossRef: [Author and Title](#)
Google Scholar: [Author Only](#) [Title Only](#) [Author and Title](#)

Lof, M.E., Gee, M., Dicke, M., Gort, G., and Hemerik, L. (2013). Exploitation of Chemical Signaling by Parasitoids: Impact on Host Population Dynamics. *Journal of chemical ecology* 39, 752-763

Pubmed: [Author and Title](#)
CrossRef: [Author and Title](#)
Google Scholar: [Author Only](#) [Title Only](#) [Author and Title](#)

Long, S. P., and Naidu, S.L. (2002). Effects of oxidants at the biochemical, cell, and physiological levels, with particular reference to ozone, pp. 69-88, in J. N. B. Bell and M. Treshow (eds.). *Air Pollution and Plant Life*. Wiley, London.

Pubmed: [Author and Title](#)
CrossRef: [Author and Title](#)
Google Scholar: [Author Only](#) [Title Only](#) [Author and Title](#)

Ludwikow, A., and Sadowski, J. (2008). Gene networks in plant ozone stress response and tolerance. *Journal of Integrative Plant Biology*. 50, 1256-1267.

Pubmed: [Author and Title](#)
CrossRef: [Author and Title](#)
Google Scholar: [Author Only](#) [Title Only](#) [Author and Title](#)

Martin, M.V.V., Fiol, D.F., Sundaresan, V., Zabaleta, E.J., and Pagnussat, G.C. (2013). oiwa, a female gametophytic mutant impaired in a mitochondrial manganese-superoxide dismutase, reveals crucial roles for reactive oxygen species during embryo sac development and fertilization in Arabidopsis. *The Plant Cell* 25, 1573-1591.

Pubmed: [Author and Title](#)
CrossRef: [Author and Title](#)

Google Scholar: [Author Only](#) [Title Only](#) [Author and Title](#)

McCormick, A.J., and Kruger, N.J. (2015). Lack of fructose 2,6-bisphosphate compromises photosynthesis and growth in Arabidopsis in fluctuating environments. The Plant journal : for cell and molecular biology 81, 670-683.

Pubmed: [Author and Title](#)

CrossRef: [Author and Title](#)

Google Scholar: [Author Only](#) [Title Only](#) [Author and Title](#)

McGrath, K.C., Dombrecht, B., and Manners, J.M. (2005). Repressor-and activator-type ethylene response factors functioning in jasmonate signaling and disease resistance identified via a genome-wide screen of Arabidopsis transcription factor gene expression. Plant Physiology 139, 949-59.

Pubmed: [Author and Title](#)

CrossRef: [Author and Title](#)

Google Scholar: [Author Only](#) [Title Only](#) [Author and Title](#)

McKenna, M.C., Waagepetersen, H.S., Schousboe, A., and Sonnewald, U. (2006). Neuronal and astrocytic shuttle mechanisms for cytosolic-mitochondrial transfer of reducing equivalents: current evidence and pharmacological tools. Biochemical pharmacology 71, 399-407.

Pubmed: [Author and Title](#)

CrossRef: [Author and Title](#)

Google Scholar: [Author Only](#) [Title Only](#) [Author and Title](#)

Meldau, S., Erb, M., and Baldwin, I.T. (2012). Defence on demand: mechanisms behind optimal defence patterns. Annals of Botany 110, 1503-1514.

Pubmed: [Author and Title](#)

CrossRef: [Author and Title](#)

Google Scholar: [Author Only](#) [Title Only](#) [Author and Title](#)

Michaeli, S., and Fromm, H. (2015). Closing the loop on the GABA shunt in plants: are GABA metabolism and signaling entwined? Frontiers in plant science 6, 419.

Pubmed: [Author and Title](#)

CrossRef: [Author and Title](#)

Google Scholar: [Author Only](#) [Title Only](#) [Author and Title](#)

Mirabella, R., Rauwerda, H., Allmann, S., Scala, A., Spyropoulou, E.A., de Vries, M., Boersma, M.R., Breit, T.M., Haring, M.A., and Schuurink, R.C. (2015). WRKY40 and WRKY6 act downstream of the green leaf volatile E-2-hexenal in Arabidopsis. The Plant journal : for cell and molecular biology 83, 1082-1096.

Pubmed: [Author and Title](#)

CrossRef: [Author and Title](#)

Google Scholar: [Author Only](#) [Title Only](#) [Author and Title](#)

Misra, P., Pandey, A., Tiwari, M., Chandrashekar, K., Sidhu, O.P., Asif, M.H., Chakrabarty, D., Singh, P.K., Trivedi, P.K., Nath, P., and Tuli, R. (2010). Modulation of transcriptome and metabolome of tobacco by Arabidopsis transcription factor, AtMYB12, leads to insect resistance. Plant physiology 152, 2258-2268.

Pubmed: [Author and Title](#)

CrossRef: [Author and Title](#)

Google Scholar: [Author Only](#) [Title Only](#) [Author and Title](#)

Missihoun, T.D., Hou, Q., Mertens, D., and Bartels, D. (2014). Sequence and functional analyses of the aldehyde dehydrogenase 7B4 gene promoter in Arabidopsis thaliana and selected Brassicaceae: regulation patterns in response to wounding and osmotic stress. Planta 239, 1281-1298.

Pubmed: [Author and Title](#)

CrossRef: [Author and Title](#)

Google Scholar: [Author Only](#) [Title Only](#) [Author and Title](#)

Mittler, R. (2006). Abiotic stress, the field environment and stress combination. Trends in Plant Science 11, 15-19.

Pubmed: [Author and Title](#)

CrossRef: [Author and Title](#)

Google Scholar: [Author Only](#) [Title Only](#) [Author and Title](#)

Morandini, P. (2013). Control limits for accumulation of plant metabolites: brute force is no substitute for understanding. Plant biotechnology journal 11, 253-267.

Pubmed: [Author and Title](#)

CrossRef: [Author and Title](#)

Google Scholar: [Author Only](#) [Title Only](#) [Author and Title](#)

Mráček, T., Drahotka, Z., and Houštek, J. (2013). The function and the role of the mitochondrial glycerol-3-phosphate dehydrogenase in mammalian tissues. Biochimica et biophysica acta 1827, 401-410.

Pubmed: [Author and Title](#)

CrossRef: [Author and Title](#)

Google Scholar: [Author Only](#) [Title Only](#) [Author and Title](#)

Mueller, S.P., Krause, D.M., Mueller, M.J., and Fekete, A. (2015). Accumulation of extra-chloroplastic triacylglycerols in Arabidopsis seedlings during heat acclimation. Journal of Experimental Botany 66, 4517-4526.

Pubmed: [Author and Title](#)

CrossRef: [Author and Title](#)

Google Scholar: [Author Only](#) [Title Only](#) [Author and Title](#)

Mulaudzi, T., Ludidi, N., Ruzvidzo, O., Morse, M., Hendricks, N., Iwuoha, E., and Gehring, C. (2011). Identification of a novel Arabidopsis thaliana nitric oxide-binding molecule with guanylate cyclase activity in vitro. FEBS letters 585, 2693-2697.

Pubmed: [Author and Title](#)
CrossRef: [Author and Title](#)
Google Scholar: [Author Only](#) [Title Only](#) [Author and Title](#)

Murata, N., Takahashi, S., Nishiyama, Y., and Allakhverdiev, S.I. (2007). Photoinhibition of photosystem II under environmental stress. *Biochimica et biophysica acta* 1767, 414-421.

Pubmed: [Author and Title](#)
CrossRef: [Author and Title](#)
Google Scholar: [Author Only](#) [Title Only](#) [Author and Title](#)

Nabity, P.D., Zavala, J.A., and DeLucia, E.H. (2012). Herbivore induction of jasmonic acid and chemical defences reduce photosynthesis in *Nicotiana attenuata*. *Journal of Experimental Botany* 64.

Pubmed: [Author and Title](#)
CrossRef: [Author and Title](#)
Google Scholar: [Author Only](#) [Title Only](#) [Author and Title](#)

Nakabayashi, R. and Saito, K. (2015). Integrated metabolomics for abiotic stress responses in plants. *Current Opinion in Plant Biology* 24, 10-16.

Pubmed: [Author and Title](#)
CrossRef: [Author and Title](#)
Google Scholar: [Author Only](#) [Title Only](#) [Author and Title](#)

Nambara, E., Kawaide, H., Kamiya, Y., and Naito, S. (1998). Characterization of an *Arabidopsis thaliana* mutant that has a defect in ABA accumulation: ABA-dependent and ABA-independent accumulation of free amino acids during dehydration. *Plant and Cell Physiology* 39, 853-858.

Pubmed: [Author and Title](#)
CrossRef: [Author and Title](#)
Google Scholar: [Author Only](#) [Title Only](#) [Author and Title](#)

Nielsen, T., Rung, J., and Villadsen, D. (2004). Fructose-2, 6-bisphosphate: a traffic signal in plant metabolism. *Trends in plant science* 9, 556-563.

Pubmed: [Author and Title](#)
CrossRef: [Author and Title](#)
Google Scholar: [Author Only](#) [Title Only](#) [Author and Title](#)

Niyogi, K.K. (2000). Safety valves for photosynthesis. *Current opinion in plant biology* 3, 455-460.

Pubmed: [Author and Title](#)
CrossRef: [Author and Title](#)
Google Scholar: [Author Only](#) [Title Only](#) [Author and Title](#)

Noctor, G., De Paepe, R., and Foyer, C.H. (2007). Mitochondrial redox biology and homeostasis in plants. *Trends in plant science* 12, 125-134.

Pubmed: [Author and Title](#)
CrossRef: [Author and Title](#)
Google Scholar: [Author Only](#) [Title Only](#) [Author and Title](#)

Nunes-Nesi, A., Sulpice, R., Gibon, Y., and Fernie, A.R. (2008). The enigmatic contribution of mitochondrial function in photosynthesis. *Journal of Experimental Botany* 59, 1675-1684.

Pubmed: [Author and Title](#)
CrossRef: [Author and Title](#)
Google Scholar: [Author Only](#) [Title Only](#) [Author and Title](#)

Onkokesung, N., Reichelt, M., van Doorn, A., Schuurink, R.C., van Loon, J., and Dicke, M. (2014). Modulation of flavonoid metabolites in *Arabidopsis thaliana* through overexpression of the MYB75 transcription factor: role of kaempferol-3,7-dirhamnoside in resistance to the specialist insect herbivore *Pieris brassicae*. *Journal of Experimental Botany* 65, 2203-2217.

Pubmed: [Author and Title](#)
CrossRef: [Author and Title](#)
Google Scholar: [Author Only](#) [Title Only](#) [Author and Title](#)

Ortiz-Lopez, A., Chang, H.C., and Bush, D.R. (2000). Amino acid transporters in plants. *Biochimica et Biophysica Acta (BBA) - Biomembranes* 1465, 275-280.

Pubmed: [Author and Title](#)
CrossRef: [Author and Title](#)
Google Scholar: [Author Only](#) [Title Only](#) [Author and Title](#)

Paoletti E., Grulke N.E. (2005). Does living in elevated CO₂ ameliorate tree response to ozone? A review on stomatal responses. *Environmental Pollution* 137, 483-93.

Pubmed: [Author and Title](#)
CrossRef: [Author and Title](#)
Google Scholar: [Author Only](#) [Title Only](#) [Author and Title](#)

Pandey, P., Ramegowda, V., Senthil-Kumar, M. (2015). Shared and unique responses of plants to multiple individual stresses and stress combinations: physiological and molecular mechanisms. *Frontiers in Plant Science* 6, 723.

Pubmed: [Author and Title](#)
CrossRef: [Author and Title](#)
Google Scholar: [Author Only](#) [Title Only](#) [Author and Title](#)

Pieterse, C.M.J., van der Does, D., Zamioudis, C., Leon-Reyes, A., van Wees, S.C.M. (2012) Hormonal Modulation of Plant Immunity. *Annual Review of Cell Developmental Biology* 28, 489-521.

Pubmed: [Author and Title](#)
CrossRef: [Author and Title](#)

Google Scholar: [Author Only](#) [Title Only](#) [Author and Title](#)

Persak, H., and Pitzschke, A. (2013). Tight interconnection and multi-level control of Arabidopsis MYB44 in MAPK cascade signalling. Plos One 8.

Pubmed: [Author and Title](#)

CrossRef: [Author and Title](#)

Google Scholar: [Author Only](#) [Title Only](#) [Author and Title](#)

Persak, H., and Pitzschke, A. (2014). Dominant repression by Arabidopsis transcription factor MYB44 causes oxidative damage and hypersensitivity to abiotic stress. International journal of molecular sciences 15, 2517-2537.

Pubmed: [Author and Title](#)

CrossRef: [Author and Title](#)

Google Scholar: [Author Only](#) [Title Only](#) [Author and Title](#)

Petersen, B., Chen, S., Hansen, C., Olsen, C., and Halkier, B. (2002). Composition and content of glucosinolates in developing Arabidopsis thaliana. Planta 214, 562-571.

Pubmed: [Author and Title](#)

CrossRef: [Author and Title](#)

Google Scholar: [Author Only](#) [Title Only](#) [Author and Title](#)

Pinto, D.M., Blande, J.D., Souza, S.R., Nerg, A-M., Holopainen, J.K. (2010). Plant Volatile Organic Compounds (VOCs) in Ozone (O3) Polluted Atmospheres: The Ecological Effects. Journal of Chemical Ecology 36, 22-34.

Pubmed: [Author and Title](#)

CrossRef: [Author and Title](#)

Google Scholar: [Author Only](#) [Title Only](#) [Author and Title](#)

Pitzschke, A., and Hirt, H. (2008). Disentangling the Complexity of Mitogen-Activated Protein Kinases and Reactive Oxygen Species Signaling. Plant physiology 149, 606-615.

Pubmed: [Author and Title](#)

CrossRef: [Author and Title](#)

Google Scholar: [Author Only](#) [Title Only](#) [Author and Title](#)

Poelman, E.H., Loon, J.J., Dam, N.M., Vet, L.E., and Dicke, M. (2010). Herbivore-induced plant responses in Brassica oleracea prevail over effects of constitutive resistance and result in enhanced herbivore attack. Ecological Entomology 35, 240-247.

Pubmed: [Author and Title](#)

CrossRef: [Author and Title](#)

Google Scholar: [Author Only](#) [Title Only](#) [Author and Title](#)

Potuschak, T., Lechner, E., Parmentier, Y., Yanagisawa, S., Grava, S., Koncz, C., and Genschik, P. (2003). EIN3-Dependent Regulation of Plant Ethylene Hormone Signaling by Two Arabidopsis F Box Proteins EBF1 and EBF2. Cell 115, 679-689.

Pubmed: [Author and Title](#)

CrossRef: [Author and Title](#)

Google Scholar: [Author Only](#) [Title Only](#) [Author and Title](#)

Prasch, C.M., and Sonnewald, U. (2013). Simultaneous Application of Heat, Drought, and Virus to Arabidopsis Plants Reveals Significant Shifts in Signaling Networks. Plant physiology 162, 1849-1866.

Pubmed: [Author and Title](#)

CrossRef: [Author and Title](#)

Google Scholar: [Author Only](#) [Title Only](#) [Author and Title](#)

Pré, M., Atallah, M., Champion, A., and Vos, D.M. (2008). The AP2/ERF domain transcription factor ORA59 integrates jasmonic acid and ethylene signals in plant defense. Plant Physiology 147, 1347-1357

Pubmed: [Author and Title](#)

CrossRef: [Author and Title](#)

Google Scholar: [Author Only](#) [Title Only](#) [Author and Title](#)

Provart, N., Zhu, T., (2003) A Browser-based functional classification supervisor for Arabidopsis genomics. Currents in Computational Molecular Biology, 271-272

Pubmed: [Author and Title](#)

CrossRef: [Author and Title](#)

Google Scholar: [Author Only](#) [Title Only](#) [Author and Title](#)

Quettier, A.-L.L., Shaw, E., and Eastmond, P.J. (2008). SUGAR-DEPENDENT6 encodes a mitochondrial flavin adenine dinucleotide-dependent glycerol-3-p dehydrogenase, which is required for glycerol catabolism and post germinative seedling growth in Arabidopsis. Plant physiology 148, 519-528.

Pubmed: [Author and Title](#)

CrossRef: [Author and Title](#)

Google Scholar: [Author Only](#) [Title Only](#) [Author and Title](#)

Ralph S.G., Yueh H., Friedmann M., Aeschliman D., Zeznik J.A., Nelson C.C., Butterfield Y.S., Kirkpatrick R., Liu J., Jones S.J., Marra M.A., Douglas C.J., Ritland K., Bohmann J. (2006). Conifer defence against insects: microarray gene expression profiling of Sitka spruce (Picea sitchensis) induced by mechanical wounding or feeding by spruce budworms (Choristoneura occidentalis) or white pine weevils (Pissodes strobi) reveals large-scale changes of the host transcriptome. Plant, Cell and Environment 29, 1545-1570.

Pubmed: [Author and Title](#)

CrossRef: [Author and Title](#)

Google Scholar: [Author Only](#) [Title Only](#) [Author and Title](#)

Ranieri, A., Giuntini, D., Ferraro, F., Nali, C., Baldan, B., Lorenzini, G., Soldatini, G.F., and Soldatini, F. (2001). Chronic ozone fumigation induces alterations in thylakoid functionality and composition in two poplar clones. Plant Physiology and Biochemistry

39, 999-1008.

Pubmed: [Author and Title](#)
CrossRef: [Author and Title](#)
Google Scholar: [Author Only](#) [Title Only](#) [Author and Title](#)

Renaut, J., Bohler, S., Hausman, J-F., Hoffmann, L., Sergeant, K., Ahsan, N., Jolivet, Y., and Dizengremel, P. (2009). The impact of atmospheric composition on plants: A case study of ozone and poplar. *Mass Spectrometry Reviews* 28, 495-516.

Pubmed: [Author and Title](#)
CrossRef: [Author and Title](#)
Google Scholar: [Author Only](#) [Title Only](#) [Author and Title](#)

Reymond, P., Weber, H., Damond, M., and Farmer, E.E. (2000). Differential gene expression in response to mechanical wounding and insect feeding in *Arabidopsis*. *The Plant Cell* 12, 707-720.

Pubmed: [Author and Title](#)
CrossRef: [Author and Title](#)
Google Scholar: [Author Only](#) [Title Only](#) [Author and Title](#)

Reymond, P., Bodenhausen, N., Van Poecke, R. M. P., Krishnamurthy, V., Dicke, M., Farmer, E., (2004). A conserved transcript pattern in response to a specialist and a generalist herbivore. *The Plant Cell Online* 16, 3132-3147.

Pubmed: [Author and Title](#)
CrossRef: [Author and Title](#)
Google Scholar: [Author Only](#) [Title Only](#) [Author and Title](#)

Rizhsky, L., Liang, H., Mittler, R. (2002). The combined effect of drought and heat shock on gene expression in tobacco. *Plant Physiology* 130, 1143-1151.

Pubmed: [Author and Title](#)
CrossRef: [Author and Title](#)
Google Scholar: [Author Only](#) [Title Only](#) [Author and Title](#)

Rizhsky, L., Liang, H., Shuman, J., Shulaev, V., Davletova, S., and Mittler, R. (2004). When defense pathways collide. The response of *Arabidopsis* to a combination of drought and heat stress. *Plant Physiology* 134, 1683-1696.

Pubmed: [Author and Title](#)
CrossRef: [Author and Title](#)
Google Scholar: [Author Only](#) [Title Only](#) [Author and Title](#)

Rolland F., Baena-Gonzalez E., Sheen J. (2006). Sugar sensing and signaling in plants: conserved and novel mechanisms. *Annual Review of Plant Biology*. 57, 675-709.

Pubmed: [Author and Title](#)
CrossRef: [Author and Title](#)
Google Scholar: [Author Only](#) [Title Only](#) [Author and Title](#)

Saito, S., Hirai, N., Matsumoto, C., Ohgashi, H., Ohta, D., Sakata, K., and Mizutani, M. (2004). *Arabidopsis* CYP707As encode (+)-abscisic acid 8'-hydroxylase, a key enzyme in the oxidative catabolism of abscisic acid. *Plant physiology* 134, 1439-1449.

Pubmed: [Author and Title](#)
CrossRef: [Author and Title](#)
Google Scholar: [Author Only](#) [Title Only](#) [Author and Title](#)

Saito, K., Hirai, M.Y., and Yonekura-Sakakibara, K. (2008). Decoding genes with coexpression networks and metabolomics-'majority report by precogs'. *Trends in plant science* 13, 36-43.

Pubmed: [Author and Title](#)
CrossRef: [Author and Title](#)
Google Scholar: [Author Only](#) [Title Only](#) [Author and Title](#)

Saito, K., and Matsuda, F. (2010). Metabolomics for Functional Genomics, Systems Biology, and Biotechnology. *Annual review of plant biology* 61, 463-489.

Pubmed: [Author and Title](#)
CrossRef: [Author and Title](#)
Google Scholar: [Author Only](#) [Title Only](#) [Author and Title](#)

Sakaki, T., Saito, K., Kawaguchi, A., Kondo, N., and Yamada, M. (1990). Conversion of monogalactosyldiacylglycerols to triacylglycerols in ozone-fumigated spinach leaves. *Plant physiology* 94, 766-772.

Pubmed: [Author and Title](#)
CrossRef: [Author and Title](#)
Google Scholar: [Author Only](#) [Title Only](#) [Author and Title](#)

Sakurai, N., Ara, T., Ogata, Y., Sano, R., Ohno, T., Sugiyama, K., Hiruta, A., Yamazaki, K., Yano, K., Aoki, K., Aharoni, A., Hamada, K., Yokoyama, K., Kawamura, S., Otsuka, H., Tokimatsu, T., Kanehisa, M., Suzuki, H., Saito, K., and Shibata, D. (2011). KaPPA-View4: a metabolic pathway database for representation and analysis of correlation networks of gene co-expression and metabolite co-accumulation and omics data. *Nucleic acids research* 39, 677-684.

Pubmed: [Author and Title](#)
CrossRef: [Author and Title](#)
Google Scholar: [Author Only](#) [Title Only](#) [Author and Title](#)

Salvatori, E., Fusaro, L., Strasser, R.J., Bussotti, F., and Manes, F. (2015). Effects of acute O₃ stress on PSII and PSI photochemistry of sensitive and resistant snap bean genotypes (*Phaseolus vulgaris* L.), probed by prompt chlorophyll "a" fluorescence and 820 nm modulated reflectance. *Plant Physiology and Biochemistry* 97, 368-377.

Pubmed: [Author and Title](#)
CrossRef: [Author and Title](#)
Google Scholar: [Author Only](#) [Title Only](#) [Author and Title](#)

Sardans, J., Peñuelas, J., and Rivas-Ubach, A. (2011). Ecological metabolomics: overview of current developments and future challenges. *Chemoecology* 21, 191-225.

Pubmed: [Author and Title](#)

CrossRef: [Author and Title](#)

Google Scholar: [Author Only](#) [Title Only](#) [Author and Title](#)

Sawada H., Kohno Y. (2009). Differential ozone sensitivity of rice cultivars as indicated by visible injury and grain yield. *Plant Biology* 11, 70-75.

Pubmed: [Author and Title](#)

CrossRef: [Author and Title](#)

Google Scholar: [Author Only](#) [Title Only](#) [Author and Title](#)

Scheibe, R., Backhausen, J.E., Emmerlich, V., and Holtgreffe, S. (2005). Strategies to maintain redox homeostasis during photosynthesis under changing conditions. *Journal of Experimental Botany* 56, 1481-1489.

Pubmed: [Author and Title](#)

CrossRef: [Author and Title](#)

Google Scholar: [Author Only](#) [Title Only](#) [Author and Title](#)

Schwachtje, J., and Baldwin, I.T. (2008). Why does herbivore attack reconfigure primary metabolism? *Plant physiology* 146, 845-851.

Pubmed: [Author and Title](#)

CrossRef: [Author and Title](#)

Google Scholar: [Author Only](#) [Title Only](#) [Author and Title](#)

Schön, M., Toller, A., Diezel, C., Roth, C., Westphal, L., Wiermer, M., and Somssich, I.E. (2013). Analyses of wrky18 wrky40 plants reveal critical roles of SA/EDS1 signaling and indole-glucosinolate biosynthesis for *Golovinomyces orontii* resistance and a loss-of resistance towards *Pseudomonas syringae* pv. tomato AvrRPS4. *Molecular plant-microbe interactions : MPMI* 26, 758-767.

Pubmed: [Author and Title](#)

CrossRef: [Author and Title](#)

Google Scholar: [Author Only](#) [Title Only](#) [Author and Title](#)

Sclep, G., Allemeersch, J., Liechti, R., De Meyer, B., Beynon, J., Bhalerao, R., Moreau, Y., Nietfeld, W., Renou, J-P., Reymond, P., Kuiper, M. T. R., Hilson, P. (2007). CATMA, a comprehensive genome-scale resource for silencing and transcript profiling of *Arabidopsis* genes. *BMC Bioinformatics* 8, 1-13.

Pubmed: [Author and Title](#)

CrossRef: [Author and Title](#)

Google Scholar: [Author Only](#) [Title Only](#) [Author and Title](#)

Settele, J., Scholes, R., Betts, S., Bunn, S., Leadley, P., Nepstad, D., Overpeck, J.T., and Taboada, M.A. (2014). Terrestrial and inland water systems. In: *Climate Change 2014: Impacts, Adaptations and Vulnerability. Part A: Global and Sectoral Aspects. Contribution of Working Group II to the Fifth Assessment Report of the Intergovernmental Panel on Climate Change*. Cambridge University Press, Cambridge, United Kingdom and New York, NY, USA, 271-359.

Pubmed: [Author and Title](#)

CrossRef: [Author and Title](#)

Google Scholar: [Author Only](#) [Title Only](#) [Author and Title](#)

Sengupta, D., Naik, D., and Reddy, A.R. (2015). Plant aldo-keto reductases (AKRs) as multi-tasking soldiers involved in diverse plant metabolic processes and stress defense: A structure-function update. *Journal of plant physiology* 179, 40-55.

Pubmed: [Author and Title](#)

CrossRef: [Author and Title](#)

Google Scholar: [Author Only](#) [Title Only](#) [Author and Title](#)

Shao, Y., Jiang, J., Ran, L., Lu, C., Wei, C., and Wang, Y. (2014). Analysis of Flavonoids and Hydroxycinnamic Acid Derivatives in Rapeseeds (*Brassica napus* L. var. napus) by HPLC-PDA-ESI(-)-MSn/HRMS. *Journal of agricultural and food chemistry* 62, 2935-2945.

Pubmed: [Author and Title](#)

CrossRef: [Author and Title](#)

Google Scholar: [Author Only](#) [Title Only](#) [Author and Title](#)

Sharma, Y.K., Leon, J., Raskin, I., and Davis, K.R. (1996). Ozone-induced responses in *Arabidopsis thaliana*: The role of salicylic acid in the accumulation of defense-related transcripts and induced resistance. *Proceedings of the National Academy of Sciences of the United States of America* 93, 5099-5104.

Pubmed: [Author and Title](#)

CrossRef: [Author and Title](#)

Google Scholar: [Author Only](#) [Title Only](#) [Author and Title](#)

Shelp, B.J., Bown, A.W., and Faure, D. (2006). Extracellular gamma-aminobutyrate mediates communication between plants and other organisms. *Plant physiology* 142, 1350-1352.

Pubmed: [Author and Title](#)

CrossRef: [Author and Title](#)

Google Scholar: [Author Only](#) [Title Only](#) [Author and Title](#)

Shen, W., Wei, Y., Dauk, M., Zheng, Z., and Zou, J. (2003). Identification of a mitochondrial glycerol-3-phosphate dehydrogenase from *Arabidopsis thaliana*: evidence for a mitochondrial glycerol-3-phosphate shuttle in plants. *FEBS letters* 536, 92-96.

Pubmed: [Author and Title](#)

CrossRef: [Author and Title](#)

Google Scholar: [Author Only](#) [Title Only](#) [Author and Title](#)

Shen, W., Wei, Y., Dauk, M., Tan, Y., Taylor, D.C., Selvaraj, G., and Zou, J. (2006). Involvement of a Glycerol-3-Phosphate Dehydrogenase in Modulating the NADH/NAD⁺ Ratio Provides Evidence of a Mitochondrial Glycerol-3-Phosphate Shuttle in *Arabidopsis*. *The Plant Cell* 18, 422-441.

Pubmed: [Author and Title](#)
CrossRef: [Author and Title](#)
Google Scholar: [Author Only](#) [Title Only](#) [Author and Title](#)

Shim, J.S., Jung, C., Lee, S., Min, K., Lee, Y.-W.W., Choi, Y., Lee, J.S., Song, J.T., Kim, J.-K.K., and Choi, Y.D. (2013). AtMYB44 regulates WRKY70 expression and modulates antagonistic interaction between salicylic acid and jasmonic acid signaling. The Plant journal : for cell and molecular biology 73, 483-495.

Pubmed: [Author and Title](#)
CrossRef: [Author and Title](#)
Google Scholar: [Author Only](#) [Title Only](#) [Author and Title](#)

Shulaev, V., Cortes, D., Miller, G., and Mittler, R. (2008). Metabolomics for plant stress response. Physiologia plantarum 132, 199-208.

Pubmed: [Author and Title](#)
CrossRef: [Author and Title](#)
Google Scholar: [Author Only](#) [Title Only](#) [Author and Title](#)

Singh E., Tiwari S., Agrawal M. (2009). Effects of elevated ozone on photosynthesis and stomatal conductance of two soybean varieties: a case study to assess impacts of one component of predicted global climate change. Plant Biology 11,101-108.

Pubmed: [Author and Title](#)
CrossRef: [Author and Title](#)
Google Scholar: [Author Only](#) [Title Only](#) [Author and Title](#)

Simmonds, M.S. (2003). Flavonoid-insect interactions: recent advances in our knowledge. Phytochemistry 64, 21-30.

Pubmed: [Author and Title](#)
CrossRef: [Author and Title](#)
Google Scholar: [Author Only](#) [Title Only](#) [Author and Title](#)

Smallegange, R. C., van Loon, J. J. A., Blatt, S. E, Harvey J. A., Agerbirk N., Dicke M. (2007). Flower vs. Leaf Feeding by Pieris brassicae: Glucosinolate-Rich Flower Tissues are Preferred and Sustain Higher Growth Rate. Journal of Chemical Ecology 33, 1831-1844.

Pubmed: [Author and Title](#)
CrossRef: [Author and Title](#)
Google Scholar: [Author Only](#) [Title Only](#) [Author and Title](#)

Smyth, G.K. (2004). Linear models and empirical bayes methods for assessing differential expression in microarray experiments. Stat. Appl. Genet. Mol. Biol. 3: e3.

Pubmed: [Author and Title](#)
CrossRef: [Author and Title](#)
Google Scholar: [Author Only](#) [Title Only](#) [Author and Title](#)

Song, S., Huang, H., Gao, H., Wang, J., Wu, D., Liu, X., Yang, S., Zhai, Q., Li, C., Qi, T., and Xie, D. (2014). Interaction between MYC2 and ETHYLENE INSENSITIVE3 Modulates Antagonism between Jasmonate and Ethylene Signaling in Arabidopsis. The Plant Cell 26, 263-279.

Pubmed: [Author and Title](#)
CrossRef: [Author and Title](#)
Google Scholar: [Author Only](#) [Title Only](#) [Author and Title](#)

Song, J., Zhu, C., Zhang, X., Wen, X., Liu, L., Peng, J., Guo, H., and Yi, C. (2015). Biochemical and Structural Insights into the Mechanism of DNA Recognition by Arabidopsis ETHYLENE INSENSITIVE3. Plos One 10.

Pubmed: [Author and Title](#)
CrossRef: [Author and Title](#)
Google Scholar: [Author Only](#) [Title Only](#) [Author and Title](#)

Stam, J.M., Kroes, A, Li, Y., Gols, R., van Loon, J., Poelman, E.H., and Dicke, M. (2014). Plant Interactions with Multiple Insect Herbivores: From Community to Genes. Annual review of plant biology 65, 689-713.

Pubmed: [Author and Title](#)
CrossRef: [Author and Title](#)
Google Scholar: [Author Only](#) [Title Only](#) [Author and Title](#)

Steuer, R., (2006). Review: on the analysis and interpretation of correlations in metabolomic data. Briefing in Bioinformatics 7,151-158.

Pubmed: [Author and Title](#)
CrossRef: [Author and Title](#)
Google Scholar: [Author Only](#) [Title Only](#) [Author and Title](#)

Strehmel, N., Hummel, J., Erban, A, Strassburg, K., and Kopka, J. (2008). Retention index thresholds for compound matching in GC-MS metabolite profiling. Journal of chromatography. B, Analytical technologies in the biomedical and life sciences 871, 182-190.

Pubmed: [Author and Title](#)
CrossRef: [Author and Title](#)
Google Scholar: [Author Only](#) [Title Only](#) [Author and Title](#)

Storey, J.D., and Tibshirani, R. (2003). Statistical significance for genome-wide studies. Proceedings of the National Academy of Sciences of the United States of America 100, 9440-9445.

Pubmed: [Author and Title](#)
CrossRef: [Author and Title](#)
Google Scholar: [Author Only](#) [Title Only](#) [Author and Title](#)

Suzuki, N., Rivero, M.R., Shulaev, V., Blumwald, E., and Mittler, R. (2014) Abiotic and biotic stress combinations. New Phytologist 203, 32-43.

Pubmed: [Author and Title](#)
CrossRef: [Author and Title](#)
Google Scholar: [Author Only](#) [Title Only](#) [Author and Title](#)

Sønderby, I., Hansen, B., Bjarnholt, N., Ticconi, C., Halkier, B., and Kliebenstein, D.J. (2007). A Systems Biology Approach Identifies a R2R3 MYB Gene Subfamily with Distinct and Overlapping Functions in Regulation of Aliphatic Glucosinolates. Plos One 2.

Pubmed: [Author and Title](#)
CrossRef: [Author and Title](#)
Google Scholar: [Author Only](#) [Title Only](#) [Author and Title](#)

Tang J.Y., Zielinski R.E., Zangerl A.R., Crofts A.R., Berenbaum M.R., DeLucia E.H. (2006). The differential effects of herbivory by first and fourth instars of *Trichoplusia ni* (Lepidoptera: Noctuidae) on photosynthesis in *Arabidopsis thaliana*. Journal of Experimental Botany 57, 527-536.

Pubmed: [Author and Title](#)
CrossRef: [Author and Title](#)
Google Scholar: [Author Only](#) [Title Only](#) [Author and Title](#)

Tang, J., Zielinski, R., Aldea, M., and DeLucia, E. (2009). Spatial association of photosynthesis and chemical defense in *Arabidopsis thaliana* following herbivory by *Trichoplusia ni*. Physiologia plantarum 137, 115-124.

Pubmed: [Author and Title](#)
CrossRef: [Author and Title](#)
Google Scholar: [Author Only](#) [Title Only](#) [Author and Title](#)

Textor, S., and Gershenzon, J. (2008). Herbivore induction of the glucosinolate-myrosinase defense system: major trends, biochemical bases and ecological significance. Phytochemistry Reviews 8, 149-170.

Pubmed: [Author and Title](#)
CrossRef: [Author and Title](#)
Google Scholar: [Author Only](#) [Title Only](#) [Author and Title](#)

Thimm, O., Blasing, O., Gibon, Y., Nagel, A., Meyer, S., Kruger, P., Selbig, J., Muller, L.A., Rhee, S.Y., and Stitt, M. (2004). MAPMAN: a user-driven tool to display genomics data sets onto diagrams of metabolic pathways and other biological processes. The Plant journal : for cell and molecular biology 37, 914-939.

Pubmed: [Author and Title](#)
CrossRef: [Author and Title](#)
Google Scholar: [Author Only](#) [Title Only](#) [Author and Title](#)

Tokimatsu, T., Sakurai, N., Suzuki, H., Ohta, H., Nishitani, K., Koyama, T., Umezawa, T., Misawa, N., Saito, K., and Shibata, D. (2005). KaPPA-view: a web-based analysis tool for integration of transcript and metabolite data on plant metabolic pathway maps. Plant physiology 138, 1289-1300.

Pubmed: [Author and Title](#)
CrossRef: [Author and Title](#)
Google Scholar: [Author Only](#) [Title Only](#) [Author and Title](#)

Tsang, E.W., Bowler, C., Herouart, D., Van Camp, W., Villarroel, R., Genetello, C., Van Montagu, M., and Inze, D. (1991). Differential regulation of superoxide dismutases in plants exposed to environmental stress. The Plant Cell 3, 783-792.

Pubmed: [Author and Title](#)
CrossRef: [Author and Title](#)
Google Scholar: [Author Only](#) [Title Only](#) [Author and Title](#)

Turner, J.G., Ellis, C., and Devoto, A. (2002). The jasmonate signal pathway. The Plant Cell 14 Suppl., S153-164.

Pubmed: [Author and Title](#)
CrossRef: [Author and Title](#)
Google Scholar: [Author Only](#) [Title Only](#) [Author and Title](#)

Vahisalu, T., Puzõrjova, I., Brosché, M., and Valk, E. (2010). Ozone-triggered rapid stomatal response involves the production of reactive oxygen species, and is controlled by SLAC1 and OST1. The Plant Journal 62, 442-453.

Pubmed: [Author and Title](#)
CrossRef: [Author and Title](#)
Google Scholar: [Author Only](#) [Title Only](#) [Author and Title](#)

Vainonen, J.P., and Kangasjarvi, J. (2015). Plant signalling in acute ozone exposure. Plant, Cell and Environment 38, 240-252.

Pubmed: [Author and Title](#)
CrossRef: [Author and Title](#)
Google Scholar: [Author Only](#) [Title Only](#) [Author and Title](#)

van Dam, N.M., Witjes, L., and Svatoš, A. (2004). Interactions between aboveground and belowground induction of glucosinolates in two wild Brassica species. New Phytologist 161, 801-810.

Pubmed: [Author and Title](#)
CrossRef: [Author and Title](#)
Google Scholar: [Author Only](#) [Title Only](#) [Author and Title](#)

Van Dingenen, R., Dentener, F.J., Raes, F., Krol, M.C., Emberson, L. and Cofala, J. (2009). The global impact of ozone on agricultural crop yields under current and future air quality legislation. Atmospheric Environment. 43, 604-618.

Pubmed: [Author and Title](#)
CrossRef: [Author and Title](#)
Google Scholar: [Author Only](#) [Title Only](#) [Author and Title](#)

Warde-Farley, D., Donaldson, S.L., Comes, O., Zuberi, K., Badrawi, R., Chao, P., Franz, M., Grouios, C., Kazi, F., Lopes, C.T., Maitland, A., Mostafavi, S., Montojo, J., Shao, Q., Wright, G., Bader, G.D., and Morris, Q. (2010). The GeneMANIA prediction server: biological network integration for gene prioritization and predicting gene function. Nucleic acids research 38, 214-220.

Pubmed: [Author and Title](#)
CrossRef: [Author and Title](#)
Google Scholar: [Author Only](#) [Title Only](#) [Author and Title](#)

Watanabe, M., Balazadeh, S., Tohge, T., Erban, A., Giavalisco, P., Kopka, J., Mueller-Roeber, B., Fernie, A.R., and Hoefgen, R. (2013). Comprehensive Dissection of Spatiotemporal Metabolic Shifts in Primary, Secondary, and Lipid Metabolism during Developmental Senescence in Arabidopsis. *Plant physiology* 162, 1290-1310.

Pubmed: [Author and Title](#)
CrossRef: [Author and Title](#)
Google Scholar: [Author Only](#) [Title Only](#) [Author and Title](#)

Weckwerth, W. (2011). Green systems biology - From single genomes, proteomes and metabolomes to ecosystems research and biotechnology. *Journal of proteomics* 75, 284-305.

Pubmed: [Author and Title](#)
CrossRef: [Author and Title](#)
Google Scholar: [Author Only](#) [Title Only](#) [Author and Title](#)

Xiong, L., and Yang, Y. (2003). Disease Resistance and Abiotic Stress Tolerance in Rice Are Inversely Modulated by an Abscisic Acid-Inducible Mitogen-Activated Protein Kinase. *The Plant Cell Online* 15, 745-759.

Pubmed: [Author and Title](#)
CrossRef: [Author and Title](#)
Google Scholar: [Author Only](#) [Title Only](#) [Author and Title](#)

Xu C., Fan J., Cornish A.J., Benning C. (2008). Lipid trafficking between the endoplasmic reticulum and the plastid in Arabidopsis requires the extraplastidic TGD4 protein. *Plant Cell* 20, 2190-2204

Pubmed: [Author and Title](#)
CrossRef: [Author and Title](#)
Google Scholar: [Author Only](#) [Title Only](#) [Author and Title](#)

Yendrek, C.R., Koester R.P., Ainsworth E.A. (2015). A comparative analysis of transcriptomic, biochemical, and physiological responses to elevated ozone identifies species-specific mechanisms of resilience in legume crops. *Journal of Experimental Botany* 67, 7101-7112.

Pubmed: [Author and Title](#)
CrossRef: [Author and Title](#)
Google Scholar: [Author Only](#) [Title Only](#) [Author and Title](#)

Zangerl A R., Hamilton J. G., Miller T. J., Crofts A R., Oxborough K., Berenbaum M. R., de Lucia E. H. (2002). Impact of folivory on photosynthesis is greater than the sum of its holes. *Proceedings of the National Academy of Science* 22, 1088-1091.

Pubmed: [Author and Title](#)
CrossRef: [Author and Title](#)
Google Scholar: [Author Only](#) [Title Only](#) [Author and Title](#)

Zavala, J.A., and Baldwin, I.T. (2004). Fitness benefits of trypsin proteinase inhibitor expression in *Nicotiana attenuata* are greater than their costs when plants are attacked. *BMC Ecology* 4, 11.

Pubmed: [Author and Title](#)
CrossRef: [Author and Title](#)
Google Scholar: [Author Only](#) [Title Only](#) [Author and Title](#)

Zhang, X., Zhu, Z., An, F., Hao, D., Li, P., Song, J., Yi, C., and Guo, H. (2014). Jasmonate-Activated MYC2 Represses ETHYLENE INSENSITIVE3 Activity to Antagonize Ethylene-Promoted Apical Hook Formation in Arabidopsis. *The Plant Cell* 26, 1105-1117.

Pubmed: [Author and Title](#)
CrossRef: [Author and Title](#)
Google Scholar: [Author Only](#) [Title Only](#) [Author and Title](#)